Photochemistry and Photobiology, 2018, 94: 36–51

Photophysical and Photochemical Properties of Naturally Occurring *nor*melinonine F and Melinonine F Alkaloids and Structurally Related N(2)- and/or N(9)-methyl-β-carboline Derivatives

Federico A. O. Rasse-Suriani[1,2], Fernando S. García-Einschlag[2], Matías Rafti[2], Tobías Schmidt De León[3,4], Pedro M. David Gara[5], Rosa Erra-Balsells*[3,4] and Franco M. Cabrerizo*[1]

[1]Instituto de Investigaciones Biotecnológicas – Instituto Tecnológico de Chascomús (IIB-INTECH), Universidad Nacional de San Martín (UNSAM) – Consejo Nacional de Investigaciones Científicas y Técnicas (CONICET), Chascomús, Argentina
[2]INIFTA – CONICET, Universidad Nacional de La Plata, La Plata, Argentina
[3]Facultad de Ciencias Exactas y Naturales, Departamento de Química Orgánica, Universidad de Buenos Aires, Ciudad Universitaria, Buenos Aires, Argentina
[4]Centro de Investigación en Hidratos de Carbono (CIHIDECAR - CONICET), Universidad de Buenos Aires, Ciudad Universitaria, Buenos Aires, Argentina
[5]Centro de Investigaciones Ópticas (CIOP – CONICET – CIC), Universidad Nacional de La Plata, La Plata, Argentina
Received 25 May 2017, accepted 2 July 2017, DOI: 10.1111/php.12811

ABSTRACT

In the present work, we have synthesized and fully characterized the photophysical and photochemical properties of a selected group of N-methyl-β-carboline derivatives (9-methyl-β-carbolines and iodine salts of 2-methyl- and 2,9-dimethyl-β-carbolinium) in aqueous solutions, in the pH range 4.0–14.5. Moreover, despite the quite extensive studies reported in the literature regarding the overall photophysical behavior of N-unsubstituted βCs, this work constitutes the first full and unambiguous characterization of anionic species of N-unsubstituted βCs (*nor*harmane, harmane and harmine), present in aqueous solution under highly alkaline conditions (pH > 13.0). Acid dissociation constants (K_a), thermal stabilities, room temperature UV–visible absorption and fluorescence emission and excitation spectra, fluorescence quantum yields (Φ_F) and fluorescence lifetimes (τ_F), as well as quantum yields of singlet oxygen production (Φ_Δ) have been measured for all the studied compounds. Furthermore, for the first time to our knowledge, chemometric techniques (MCR-ALS and PARAFAC) were applied on these systems, providing relevant information about the equilibria and species involved. The impact of all the foregoing observations on the biological role, as well as the potential biotechnological applications of these compounds, is discussed.

INTRODUCTION

The presence of β-carboline (βC) alkaloids has been confirmed in a vast range of phylogenetically distant species, *i.e. Rhizaria*, *Alveolata* and *Amoebozoa* (protists organisms); *Stramenopiles* (including unicellular diatoms and blue-green algae organisms) (1); *Opisthokonta* (a monophyletic clade including both the animal and fungus kingdoms, together with the eukaryotic microorganisms grouped in the paraphyletic phylum *Choanozoa*) (2–9); *Archaeplastida* (green and red algae, land plants, etc.) (10–14); *Urochordata* (ascidians) (15–17); and *Arthropoda* (insects, arachnids, etc.) (18,19).

In particular, some N-methyl-βC derivatives have been isolated from plants. This is the case of *nor*melinonine F (2-methyl-9H-pyrido[3,4-*b*]indole or 2-methyl-*nor*harmanium) and melinonine F (1,2-dimethyl-9H-pyrido[3,4-*b*]indole or 2-methyl-harmanium) that were found in the root bark of *Strychnos usambarensis* of Rwanda (12). *Nor*melinonine F was also found to be present, in a high concentration (~250 μM), in aqueous crude extract as well as in blood (coelemic fluid) of the solitary ascidian *Cnemidocarpa irene* collected in Hokkaido (Japan) (17). In the human body, endogenously synthesized βCs were detected in different tissues and body fluids (skin, human brain, cerebrospinal fluid, plasma and urine) (2–9). However, certain environmental conditions and/or dietary habits such as alcohol intake or smoking may induce a considerable increase in βCs' basal levels (2,6–9,20). The unsubstituted 1,2,3,4-tetrahydro-βCs and the unsubstituted full-aromatic *nor*harmane (9H-pyrido[3,4-b]indole; nHo) crosses the blood–brain barrier penetrating into the brain (21,22). Inside the brain, nHo is converted by certain S-adenosyl methionine-dependent N-methyltransferases to the N-methyl-βC cation named 2-methyl-*nor*harmanium (2-Me-nHo) and subsequently to the 2,9-dimethyl-*nor*harmanium cation (2,9-diMe-nHo) (23).

A broad spectrum of biological activity has been reported for N-methyl-βCs (quaternary βCs): (1) They were described as potential pathogenetic factors in Parkinson's disease (24–26). The main mechanism through which these alkaloids would exert their effect still remains elusive. In the particular case of 2,9-diMe-nHo, a neurotoxic effect was observed due to the activation of the apoptotic cascade (27,28). (2) *Nor*melinonine F and some bromo-derivatives (7-bromo-2-methyl-9H-pyrido[3,4-*b*]indole and 7-bromo-1,2-dimethyl-9H-pyrido[3,4-*b*]indole) isolated from the solitary ascidian *Cnemidocarpa irene* were found to be inhibitors of acetylcholinesterase (AchE), with activities similar to those of galantamine (an AChE inhibitor clinically used for the treatment of mild to moderate Alzheimer's disease and various other memory impairments, in particular those of vascular origin) (17). (3)

*Corresponding authors' emails: fcabrerizo@intech.gov.ar (Franco Cabrerizo) and erra@qo.fcen.uba.ar (Rosa Erra-Balsells)

9-Methyl-*nor*harmane (9-Me-nHo) could exert neuroprotective and neuron-differentiating effects (29). (4) βCs have shown to be a promising group of antimicrobial drugs (30–39). In these regards, *nor*melinonine F and melinonine F showed antimalarial activity against chloroquine and pyrimethamine-resistant *Plasmodium falciparum* K1 (40,41). In particular, *nor*melinonine F showed the highest antiparasitic effect with a very low cytotoxicity against L6 cells (selective index, SI, >1000) (40). (5) *Nor*melinonine F as well as two chloro-*nor*melinonine F derivatives (6-chloro-2-methyl-9H-pyrido[3,4-*b*]indole and 6,8-dichloro-2-methyl-9H-pyrido[3,4-*b*]indole) displayed potent cyanobacteriocidal and algicidal activity against photosynthetic aquatic organisms (*i.e. Microcystis aeruginosa*, *Synechococcus,* and *Kirchneriella contorta*) (42). (6) As it was described for other related βCs (43–45), due to their planar chemical structure, *nor*melinonine F and melinonine F interact with cell-free DNA. Such interaction involves a partial intercalation of the indolic ring of the βC molecule into the stacked base-pairs, placing the N-methylpyridinium cationic ring in a protic environment (methyl substituent at position 2 (N-2) in pyridoindole moiety) (46).

Despite the established importance of N-methyl-βCs for the abovedescribed biological processes, molecular basis of the mechanisms involved remains unclear. If further insight is to be gained, then fundamental aspects related to spectroscopic, chemical and photophysical properties of N-methyl-βCs need to be addressed. It is known that for βCs, the latter properties strongly depend on molecular structure, as well as on the nature of the environment (solvent) and pH (47–52). To the best of our knowledge, only partial information regarding the spectroscopic characteristics of few quaternary βCs has been reported (46,53–55). Moreover, the characterization of the species present under highly alkaline aqueous conditions (pH > 13) is rather scarce or, in many cases, null.

In the present work, we have systematically investigated the chemical and photochemical properties of a selected group of quaternary N-methyl-β-carbolinium iodide salts (Scheme 1), in aqueous solution, paying special attention not only to the equilibrium and/or species dominant in physiologically relevant pH conditions but also under highly alkaline conditions. For the sake of comparison, data corresponding to the N-unsubstituted full-aromatic βCs (nHo, Ho and 1-methyl-7-methoxy-9Hpyrido[3,4b] indole [harmine, Ha]) and their 9-methyl derivatives were also included.

MATERIALS AND METHODS

Chemicals. *Nor*harmane (>98%), harmane (>98%) and harmine (>98%) from Sigma-Aldrich were used without further purification. N-methyl-β-carboline derivatives were synthesized, purified and characterized according to the procedure described below. Silica gel F254 was used in analytical thin-layer chromatography (TLC).

pH adjustment. The pH of βCs aqueous solutions (4–12) was adjusted by adding drops of aqueous NaOH or HCl solutions from a micropipette. The concentrations of acid and/or base solutions used for this purpose ranged from 0.1 to 2 M. The highly alkaline βCs aqueous solutions were also prepared with NaOH. In experiments using D_2O as solvent, D_2O (>99.9%; Aldrich), DCl solutions (99.5% in D_2O; Aldrich) and NaOD solutions (40 wt.% in D_2O, Aldrich) were used.

Thermogravimetric analysis (TGA). TGA of N-Me-βCs samples (~5 mg) was carried out at 20°C min^{-1} temperature ramp under N_2 atmosphere on a Q500 Thermal Analysis Instrument. TGA curves were analyzed with TA Universal Analysis software.

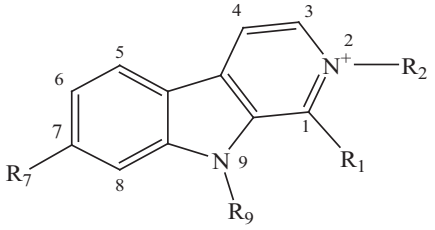

Short name, salt name (abbreviation)	R_1	R_2	R_7	R_9
*Nor*harmane (nHo)	-H	-H	-H	-H
2-Methyl-*nor*harmanium, 2-Methyl-*nor*harmanium iodide (2-Me-nHo)	-H	$-CH_3$	-H	-H
9-Methyl-*nor*harmane (9-Me-nHo)	-H	-H	-H	$-CH_3$
2,9-diMethyl-*nor*harmanium, 2,9-diMethyl-*nor*harmanium iodide (2,9-diMe-nHo)	-H	$-CH_3$	-H	$-CH_3$
Harmane (Ho)	$-CH_3$	-H	-H	-H
2-Methyl-harmanium, 2-Methyl-harmanium iodide (2-Me-Ho)	$-CH_3$	$-CH_3$	-H	-H
9-Methyl-harmane (9-Me-Ho)	$-CH_3$	-H	-H	$-CH_3$
2,9-diMethyl-harmanium, 2,9-diMethyl-harmanium iodide (2,9-diMe-Ho)	$-CH_3$	$-CH_3$	-H	$-CH_3$
Harmine (Ha)	$-CH_3$	-H	$-OCH_3$	-H
2-Methyl-harminium, 2-Methyl-harminium iodide (2-Me-Ha)	$-CH_3$	$-CH_3$	$-OCH_3$	-H
9-Methyl-harmine (9-Me-Ha)	$-CH_3$	-H	$-OCH_3$	$-CH_3$
2,9-diMethyl-harminium, 2,9-diMethyl-harminium iodide (9-Me-Ha)	$-CH_3$	$-CH_3$	$-OCH_3$	$-CH_3$

Scheme 1. Chemical structures of β-carbolines studied in the present work.

Differential scanning calorimetry (DSC). DSC experiments were carried using N-Me-βCs samples (~5 mg) loaded on hermetic platinum pans using a 20°C min^{-1} temperature ramp under N_2 atmosphere by Q2000 Thermal Analysis Instrument. DSC curves were disposed by TA Universal Analysis software.

NMR analysis. ^{1}H-NMR spectra were recorded on a Bruker 200 MHz spectrometer.

HRESI–MS analysis. High-resolution electrospray ionization (HRESI) mass spectrometry (MS) analysis was performed in positive ion mode using the mass spectrometer Q Exactive from Thermo Scientific (USA). Acquisition parameters were as follows: flow rate: 5.000 μL min^{-1}; scan range: 50–500 m/z; resolution: 140 000; sheath gas flow rate: 25 CFH; aux. gas flow rate: 0 CFH; spray voltage: 3.50 kV; S lens voltage: 50 V; capillary temp: 275°C; aux. gas heater temp: 30°C; and acquisition time: 0.5 min. Fresh methanol solutions of the analytes were used for the direct infusion and analysis. Molecular formula and monoisotopic molecular weight were obtained. Neutral compounds were detected as protonated species $[\beta C+H]^+$ (with monoisotopic atomic mass for proton = 1.007825) and then monoisotopic βC m.w. calculated. For iodine βC salts (βC^+I^-), the cation $[\beta C]^+$ was detected in straight way, and both its molecular formula and monoisotopic weight were informed. HRMS obtained are displayed in Figs. S14–S22 included in the electronic Supporting Information.

UV–visible absorption spectroscopy. Electronic absorption spectra were recorded on a Perkin-Elmer lambda 25 spectrophotometer. Measurements were made using 1 cm path length quartz cells.

Fluorescence emission spectroscopy. Steady-state fluorescence measurements were performed using a Fluoromax4 (HORIBA Jobin Yvon), whereas a single-photon-counting equipment FL3 TCSPC-SP (HORIBA Jobin Yvon) spectrofluorometer was used for time-resolved measurements. Corrected fluorescence spectra were recorded in a 1 × 1 cm path lengths quartz cell at room temperature.

Fluorescence quantum yields (Φ_F) were determined from the corrected fluorescence spectra, integrated over the entire emission profile and were calculated as the average of Φ_F values obtained using different excitation wavelengths over the entire range of the lowest-energy absorption band. The standard used was quinine sulfate at pH 4 ($\Phi_F = 0.52 \pm 0.02$) (56). To avoid inner filter effects, the absorbance of the solutions at the excitation wavelength was kept below 0.10.

Singlet oxygen production. Quantum yields of photosensitized singlet oxygen production, Φ_Δ, were obtained using the third harmonic of a Q-switched Nd-YAG laser as the excitation source (λ_{exc} = 355 nm, Surelite II- Continuum), looking at the 1270 nm $^1O_2$ phosphorescence. The orthogonal-emitted near-IR $^1O_2$ luminescence was observed through a 5 mm thick antireflective-coated silicon metal filter with a wavelength pass >1.1 μm and an interference filter at 1.27 μm by means of a preamplified (low impedance) Ge-photodiode (Applied Detector Corporation, resolution time of 1 μs). Measurements were performed in air-equilibrated D_2O solutions. The average of signals generated by 128 laser shots was recorded to improve the signal-to-noise ratio. Single exponential analysis of emission decays was performed with the exclusion of the initial part of the signal. Φ_Δ was determined by measuring its phosphorescence intensity using an optically matched solution of a reference sensitizer (perinaphthenone-2-sulfonic acid in deuterated water with $\Phi_\Delta = 0.97 \pm 0.05$) (57).

Chemometric analysis—MCR-ALS. We used curve resolution techniques, described elsewhere (58), to retrieve, from the absorbance matrix A($i \times j$), estimates of the concentration and spectral profiles. Briefly, the popular alternating least-squares (ALS) algorithm (59) is based on the iterative application of the following matrix product: $\mathbf{A = CS^T + E}$, where $\mathbf{C}(i \times n)$ is the matrix of the concentrations profiles; $\mathbf{S^T}(n \times j)$ is that containing the spectral profiles and $\mathbf{E}(i \times j)$ represents the error matrix. The indexes i, n and j denote the sampling pHs, absorbing species and recorded wavelengths, respectively. At early stages of the deconvolution process, rotational and scale ambiguities (60) were reduced by imposing non-negativity, unimodality and closure constraints (61). However, as rotational and scale ambiguities cannot be completely eliminated by this soft-modeling approach, many sets of concentration profiles and pure spectra can reproduce the initial data set with equal fit (62,63). Therefore, the preliminary model was further refined. During a second iterative stage, in addition to the non-negativity constraint imposed to the spectral profiles, the concentration profiles were forced to satisfy acid/base distribution functions (*i.e.* a hard constraint). Throughout this hybrid (soft-hard) modeling stage (64), the value of the pK_a was considered a fitting parameter whose optimal value, at each iteration step, was obtained by nonlinear regression until the ALS algorithm converged. Hence, the refined model yielded not only the individual spectral profiles associated with each acid/base species, but also the optimal pK_a values for the studied equilibria and the corresponding distribution functions.

Chemometric analysis—PARAFAC. Multivariate analysis techniques are increasingly used to obtain quantitative information from spectrofluorometric data. Parallel factor analysis (PARAFAC), the most widely used technique, is able to retrieve the information contained in complex sets of excitation–emission matrices (EEMs) (65) into independent factors, for both quantitative and qualitative analyses (66,67). PARAFAC is a generalization of principal components analysis (PCA) and has been frequently applied for the analysis of sets of EEMs arranged in three-way arrays (**X**). Mathematically, the PARAFAC model can be represented as $x_{ijk} = \sum_{f=1}^{F} a_{if} b_{jf} c_{kf} + e_{ijk}$, where $\boldsymbol{x_{ijk}}$ are the elements of **X**, the scalars $\boldsymbol{i}$, $\boldsymbol{j}$, $\boldsymbol{k}$ and $\boldsymbol{f}$ are the indexes associated with the samples, the emission wavelengths, the excitation wavelengths and the factors that contribute to the recorded signals, respectively. The values of $\boldsymbol{e_{ijk}}$ are the part of the data not explained by the model. Then, given a structure X, containing the EEMs measures for several samples, the PARAFAC algorithm decomposes **X** into three matrices **A** (scores), **B** (emission loadings) and **C** (excitation loadings). The latter matrices contain the relative contribution profiles (A), the normalized emission spectra (B) and the normalized excitation spectra (C) for each of the factors that contribute to the observed signals in the analyzed solutions. One of the main advantages of this model is that PARAFAC solution is often unique. Hence, if the data follow a PARAFAC model, then the emission loadings are not just abstract orthogonal emission profiles as would be the case in PCA. Instead, the loadings are actually estimates of the real emission spectra of the real fluorophores. PARAFAC analysis was conducted using non-negativity constraints, thus allowing only chemically relevant results. Three preprocessing steps were adopted as follows: (1) for correcting primary and secondary inner filter effects, the absorption spectra of the samples were used (68); (2) the EEMs of control solutions of Milli-Q water, adjusted to the same pH of each sample, were used for blank corrections; and (3) Rayleigh and Raman scattering signals were removed according to the protocol described by Bahram *et al.* (69). PARAFAC models from two to six factors were developed for the three-way arrays containing the EEMs at different pH values. The correct number of factors was assessed by the analysis of the physical sense of spectral loadings and by the evaluation of the distribution of residuals.

Synthesis of 2-Methyl-β-carboline iodines (2-Me-nHo, 2-Me-Ho and 2-Me-Ha). A mixture of the starting βC (nHo, Ho or Ha, respectively) (0.1 g, 0.6 mmol) and anhydrous methanol (8 mL) was placed in a stoppered balloon and stirred at room temperature until clear. Then an excess of ICH_3 was added (ratio 50:1 mol mol^{-1}, ICH_3:βC), and the mixture was kept in the dark for 24 h with stirring. The progress of the reaction was monitored by TLC. When the reaction was complete, crystals of 2-Me-βC were obtained. Crystals were filtered off and washed 5 times with cold methanol. Upon recrystallization, yellowish crystals of 2-Me-βC iodines were obtained (approx. 0.17 g, yield 90%). The product obtained was isolated and characterized by mean of physical and spectroscopic methods. (a) *2-Me-nHo,* DSC and TGA: m.p. 217°C, decomposition range under N_2 (276–332°C); UV–vis λ_{max} (log ε) in water pH 4: 374 (3.62), 305 (4.24), 250 (4.45) and 229 (4.43) nm (these values are similar, within experimental error, to those reported by Tadokoro *et al.* (17)); δ_H(200 MHz; DMSO-d_6; Me_4Si): 11.62 (1H, s, H-N9), 9.36 (1H, s, H-1), 8.82 (1H, d, H-3), 8.65 (1H, d, H-4), 8.52 (1H, d, H-8), 7.84- 7.82 (2H, m, H-7 and H-5), 7.48 (1H, m, H-6), 4.50 (3H, s, CH_3); HRMS: cation formula $C_{12}H_{11}N_2$ with m.w. 183.09222; (b) *2-Me-Ho,* DSC and TGA: m.p. 266°C, decomposition range under N_2 (271–324°C); UV–vis λ_{max} (log ε) in water pH 4: 368 (3.54), 303 (4.15), 248 (4.37) and 232 (4.32) nm; δ_H(200 MHz; DMSO-d_6; Me_4Si): 12.81 (1H, s, H-N9), 8.64 (2H, dd, H-3 and H-8), 8.47 (1H, d, H-4), 7.80 (2H, dd, H-5 and H-7), 7.46 (1H, m, H-6), 4.37 (3H, s, CH_3-N2), 3.08 (3H, s, CH_3); HRMS: cation formula $C_{13}H_{13}N_2$ with m.w. 197.10787; (c) *2-Me-Ha,* DSC and TGA: m.p. 311°C, decomposition range under N_2 (298–344°C); UV–vis λ_{max} (log ε) in water pH 4: 360 (3.79), 324 (4.19), 248 (4.45) and 227 (4.40) nm; δ_H(200 MHz; DMSO-d_6; Me_4Si): 12.65 (1H, s, H-N9), 8.52 (2H, dd, H-3 and H-4), 8.33 (1H, d, H-5), 7.11 (1H, dd, H-8), 7.05 (1H, dd, H-6), 4.32 (3H, s, CH_3-N2), 3.96 (3H, s, OCH_3), 3.03 (3H, s, CH_3); HRMS: cation formula $C_{14}H_{15}N_2O$ with m.w. 227.11844.

Synthesis of 9-methyl-β-carbolines (9-Me-nHo, 9-Me-Ho and 9-Me-Ha). A mixture of the starting βC (nHo, Ho or Ha, respectively) (0.1 g, 0.6 mmol), NaOH (0.5 g, 12.5 mmol) and anhydrous DMSO (10 mL) was placed in a stoppered balloon and stirred at room temperature until clear. Then ICH_3 was added (ratio 1:1 mol mol^{-1}, ICH_3:βC), and the mixture stirred and refluxed for 2 h. The progress of the reaction was monitored by TLC. When the reaction was completed, the resulting solution was poured into H_2O (10 mL), and the product obtained, 9-Me-βC, was extracted with hexane (7 × 5 mL). The hexane phase was collected, washed, dried and evaporated under reduced pressure. Upon recrystallization, white crystals of 9-Me-βCs were obtained (approx. 0.09 g, yield 80%). (a) *9-Me-nHo,* DSC and TGA: m.p. 103°C, decomposition range under N_2 (100–210°C); UV–vis λ_{max} (log ε) in water pH 4: 384 (3.69), 304 (4.18), 252 (4.53), 217 (4.30) and 206 (4.37) nm; δ_H(500 MHz; DMSO-d_6; Me_4Si): 9.85 (1H, s, H-1), 9.20 (1H, d, H-3), 9.09 (1H, dd, H-5), 8.95 (1H, dd, H-4), 8.52 (1H, d, H-7), 8.45 (1H, m, H-8), 8.11 (1H, t, H-6), 3.98 (3H, s, CH_3); HRMS: formula $C_{12}H_{10}N_2$ with m.w. 182.08440. (b) *9-Me-Ho,* DSC and TGA: m.p. 76°C, decomposition range under N_2 (107–224°C); UV–vis λ_{max} (log ε) in water pH 4: 378 (3.70), 302 (4.16), 259 (4.47), 252 (4.50) 216 (4.28) and 207 (4.35) nm; δ_H(200 MHz; DMSO-d_6; Me_4Si): 8.24 (2H, m, H-3 and H-8), 8.04 (1H, d, H-4), 7.60 (2H, m, H-5 and H-7), 7.28 (1H, m, H-6), 4.21 (3H, s, CH_3-N9), 3.10 (3H, s, CH_3); HRMS: formula $C_{13}H_{12}N_2$ with m.w. 196.10005; (c) *9-Me-Ha,* DSC and TGA: m.p. 118°C, decomposition range under N_2 (139–228°C); UV–vis λ_{max} (log ε) in water pH 4: 363 (3.83), 323 (4.27), 267 (4.37, sh), 252 (4.55) and 210 (4.37) nm; δ_H(200 MHz; DMSO-d_6; Me_4Si): 8.11 (2H, dd, H-3 and H-4), 7.86 (1H, dd, H-5), 7.20 (1H, d, H-8), 6.86 (1H, dd, H-6), 4.13 (3H, s, CH_3-N9), 3.92 (3H, s, OCH_3), 3.01 (3H, s, CH_3); HRMS: formula $C_{14}H_{14}N_2O$ with m.w. 226.11061.

Synthesis of 2,9-dimethyl-β-carboline iodines (2,9-diMe-nHo, 2,9-diMe-Ho and 2,9-diMe-Ha). The synthesis approach used was identical to that above described for 2-Me-βC derivatives but using the corresponding 9-Me-βC (9-Me-nHo, 9-Me-Ho or 9-Me-Ha, respectively) as starting material (0.1 g, 0.55 mmol). Upon recrystallization, brownish crystals of the corresponding 2,9-diMe-βC iodines were obtained (approx. 0.125 g, yield 70%). (a) *2,9-diMe-nHo,* DSC and TGA: m.p. 269°C, decomposition range under N_2 (260–309°C); UV–vis λ_{max} (log ε) in water pH 4: 388 (3.58), 308 (4.18), 256 (4.45) and 223 (4.46) nm; δ_H(200 MHz; DMSO-d_6; Me_4Si): 9.66 (1H, s, H-1), 8.85 (1H, d, H-3), 8.69 (1H, dd, H-4), 8.55 (1H, dd, H-8), 7.95 (1H, d, H-7), 7.55 (1H, dd, H-6), 6.80 (1H, m, H-5), 4.51 (3H, s, CH_3), 4.11 (3H, s, CH_3); HRMS: cation formula $C_{13}H_{13}N_2$ with m.w. 197.10787; (b) *2,9-diMe-Ho,* DSC and TGA: m.p. 314°C, decomposition range under N_2 (155–350°C); UV–vis λ_{max} (log ε) in water pH 4: 382 (3.61), 306 (4.15), 260 (4.41), 255 (4.44) and 221 (4.40) nm; δ_H(200 MHz; DMSO-d_6; Me_4Si): 8.69 (2H, d, H-3 and H-8), 8.49 (1H, m, H-4), 7.89 (2H, m, H-5 and H-7), 7.49 (1H, m, H-6), 4.40 (3H, s, CH_3-N2), 4.30 (3H, s, CH_3-N9), 3.25 (3H, s, CH_3); HRMS: cation formula $C_{14}H_{15}N_2$ with m.w. 211.12352; (c) *2,9-diMe-Ha,* DSC and TGA: m.p. 338°C; UV–vis λ_{max} (log ε) in water pH 4: 368 (3.83), 327 (4.28), 262 (4.44, sh), 253 (4.52) and 225 (4.76) nm; δ_H(200 MHz; DMSO-d_6; Me_4Si): 8.62 (1H, d, H-3), 8.50 (1H, d, H-4), 8.35 (1H, d, H-5), 7.42 (1H, d, H-8), 7.09 (1H, dd, H-6), 4.34 (3H, s, CH_3-N2), 4.27 (3H, s, CH_3-N9), 3.99 (3H, s, OCH_3), 3.22 (3H, s, CH_3); HRMS: cation formula $C_{15}H_{17}N_2O$ with m.w. 241.13409.

The substantially lower values obtained for m.p. and decomposition temperatures of *9-methyl-βCs* compared to the other synthesized molecules can be rationalized by considering the effect of methylation position on molecule structure and intermolecular interactions in solid phase. For the iodide 2,9-dimethyl- and 2- methyl-substituted βCs, Coulombic and H-bond intermolecular interactions are possible, and hence, the relatively high m.p. observed. On the other hand, 9-methyl-substitutes are neutral molecules with no H-bond, accordingly, m.p. are approx. 100°C lower.

RESULTS

UV–visible absorption spectroscopy

Acid–base equilibria and UV–visible absorption spectra. The net charge of βCs depends on the pH medium as well as on the chemical nature of the substituents and their relative position on

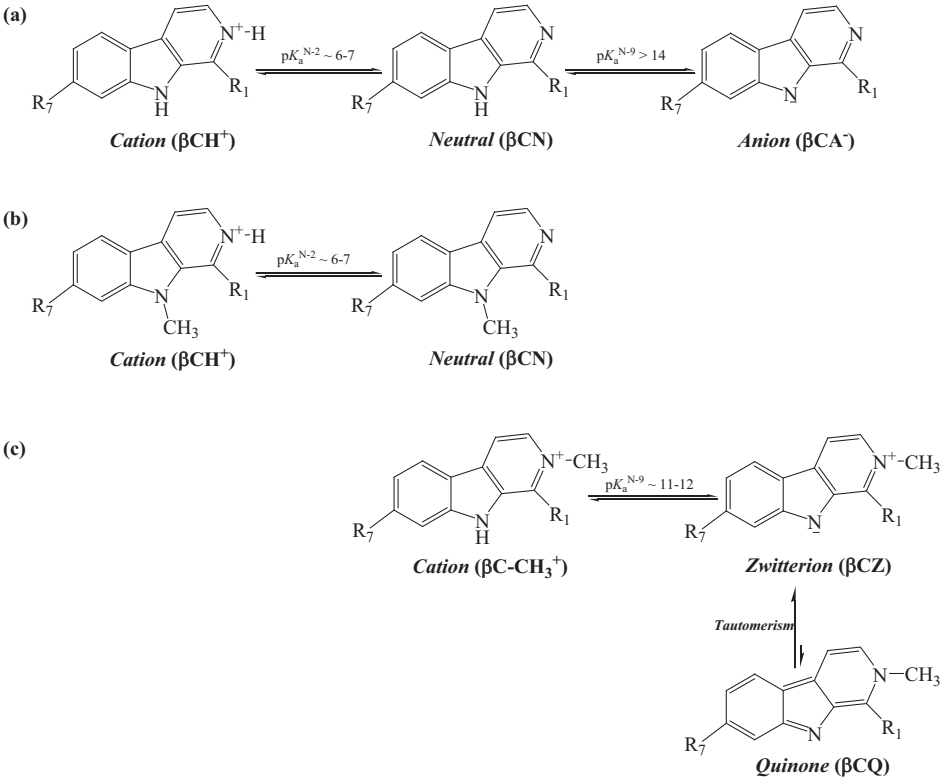

Scheme 2. Acid–base equilibria observed in aqueous solution for full-aromatic (a) N-unsubstituted βCs, (b) 9-methyl-βCs and (c) 2-methyl-βCs, in the pH range 2–14.

the main βC's ring (*vide infra*). In aqueous media, over the entire pH range, full-aromatic βCs (nHo, Ho and Ha) show two distinctive acid–base equilibria (Scheme 2a). The first one, characterized by a $pK_a^{(N\text{-}2)}$ value close to physiological pH (48,54,55,70–74), involves the protonation/deprotonation of the pyridinic nitrogen (N-2). Under highly alkaline conditions, a second equilibrium involving the protonation/deprotonation of the indolic nitrogen (N-9) is observed with an estimated $pK_a^{(N\text{-}9)}$ value higher than 14 (54,55,70–74).

Previous studies on related βCs revealed that each acid–base species has distinctive spectroscopic, physicochemical and photophysical properties (47,48). Thus, a detailed and systematic study of these properties for N-methyl-βCs in solution under different pH conditions was conducted.

To begin with, the chemical stability of acidic and alkaline aqueous solutions of 2-Me-βCs and 2,9-diMe-βCs (Scheme 1) was studied. On the contrary to what was observed for other related βC derivatives (*i.e.* chloro-harmine derivatives) (51), aqueous solutions ($2 < pH < 11$) of the investigated compounds remained stable after more than 60 days kept in cool and dark conditions (Figs. S1–S3). These results show the strong structure-dependent chemical stability of βCs.

In all the pH range studied, cationic di-N-substituted βCs did not show any acid–base equilibrium; whereas mono-N-substituted-βCs (*i.e.* 2-Me-βCs and 9-Me-βCs) showed only one reversible protonation/deprotonation equilibrium involving N-9 and N-2, respectively (Scheme 2). It is worth mentioning that the zwitterionic species produced upon N-9 deprotonation of 2-methyl-βCs (βCZ) might be involved in a tautomeric equilibrium with the corresponding anhydrous base or quinonic species (βCQ) (Scheme 2c) (53). However, in polar solvents, such as water, the latter equilibrium is displaced toward βCZ formation (75).

The corresponding absorption spectra and representative examples of spectrophotometric titration curves are shown in Fig. 1, and calculated acid dissociation equilibrium constant (K_a)

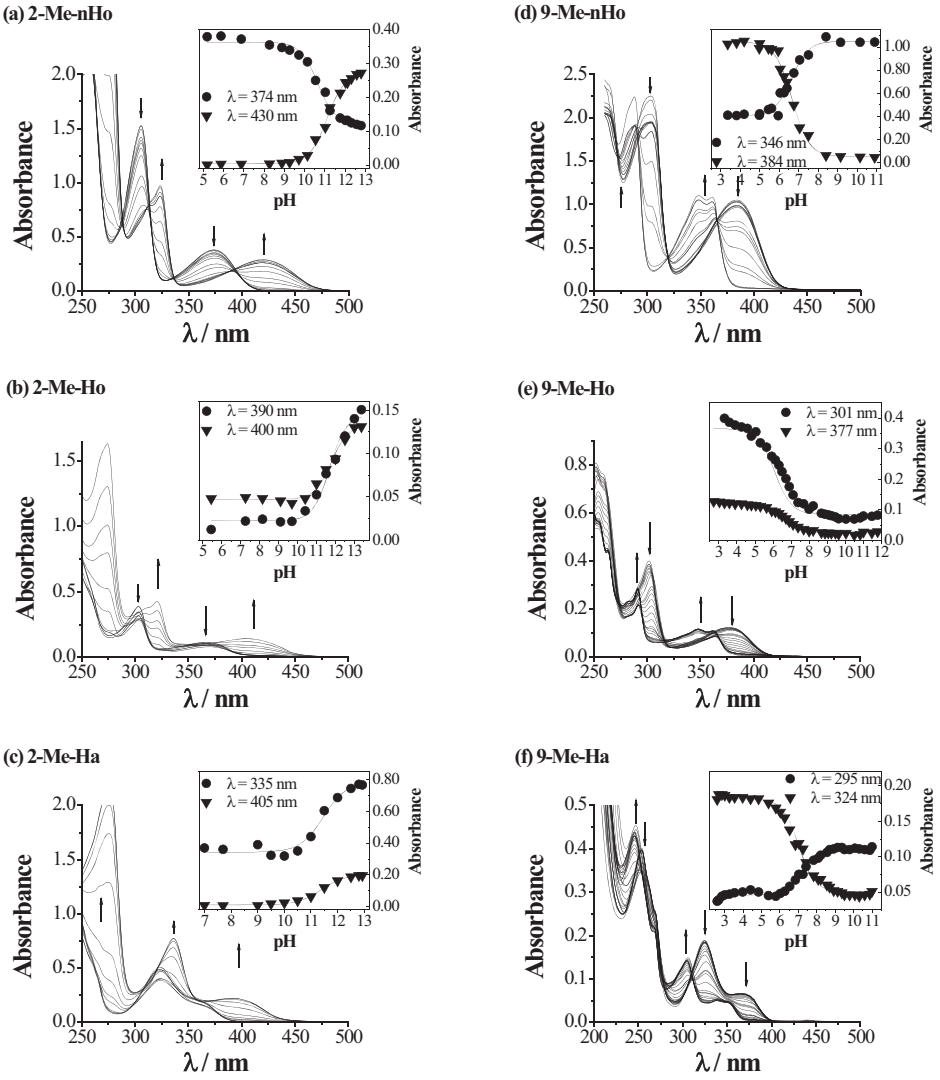

Figure 1. UV–visible spectra of 2-Me βCs (left column) and 9-Me βCs (right column) in aqueous solution recorded under different pH conditions. (a) 2-Me-nHo (80 μM), (b) 2-Me-Ho (35 μM), (c) 2-Me-Ha (34 μM), (d) 9-Me-nHo (250 μM), (e) 9-Me-Ho (25 μM) and (f) 9-Me-Ha (10 μM). In all the cases, arrows indicate the changes in band intensities as the pH increases. *Insets*: representative examples of spectrophotometric titration curves obtained at two different wavelengths (dots and triangles) and the corresponding best-fit curves (solid line).

Table 1. Summary of spectroscopic and photophysical data of the acid–base species of nHo, Ho, Ha and their N-methyl derivatives. For comparative reasons, original data obtained in the present work as well as data reported in the literature measured under identical experimental conditions are listed in black bold

Compound	pK_a in S_0[a]	pH	Species in S_0[b]	λ_{abs}/nm[c]	$\varepsilon(\lambda)/10^3$ M^{-1} cm^{-1}[d]	Species in S_1[b]	λ_F/nm[e]	Φ_F[f]	τ_F/ns[g]	Φ_Δ[h]
nHo	p$K_a^{(N-2)}$: 6.5[i], 6.85 (±0.03) [j], 7.2[m], 7.9[n]	4	βCH$^+$	**371**[v], 370[m]	**4.30**[v]	^{1}[βCH$^+$]*	**448**[v], 445[m], 450[n], 454[xx]	**0.70**[v], 0.58[xx]	**21.8**, 22.0[n], 21.2[xx]	**0.10**[v]
	p$K_a^{(N-9)}$: **14.07**[o], 14.49 (±0.07)[u], 14.5[i,m,n], 14.53 (±0.04)[j,k], 18 (±2)[j,l]	10	βCN	**337**[v] and **348**[v], 348[m]	**4.01** and **3.89**[v]	^{1}[βCN]* and ^{1}[βCH$^+$]*	**384**[v], 380[n], 385[m] **448**[v]	**0.21**[v]	**<0.5** **20.8**	**0.08**[v]
		14	βCN and βCA$^-$	**337** and **348** **381**[o], 390[m], 380[u]	**3.48**[o]	^{1}[βCA$^-$]* and	**490**[o],490[l], 450[j,u], ~460[j]	**0.03**, 0.057[u]	**9.1**	—
						^{1}[βCZ]*	**522**[o], 510[m,n], 511[j] ~520[i]		**1.9**, 1.6[n]	
2-Me-nHo	—	4	βC-CH$_3^+$	**374**, 375[n]	**4.10**	^{1}[βC-CH$_3^+$]*	**454**, 455[n]	**0.67**	**22.2**, 22.9[n]	**0.11**
	p$K_a^{(N-9)}$: **10.9** (±**0.02**), 10.9[n]	9	βC-CH$_3^+$	**374**	**4.10**	^{1}[βC-CH$_3^+$]*	**454**	**0.67**	**22.2**	
		13–14	βC-CH$_3$Z	**420**, ~420[n]	**3.06**	^{1}[βC-CH$_3$Z]*	**533**, 510[n]	**0.02**	**1.3**, 1.32[n]	—
9-Me-nHo	p$K_a^{(N-2)}$: **6.3** (±**0.3**), 6.91 ± 0.05[t]	4	βCH$^+$	**384**[v], ~390[t]	**4.84**[v]	^{1}[βCH$^+$]*	**458**[v], ~455[t]	**0.75**[v]	**23.1**[v], 23.1[t]	**0.10**[v]
	—	10	βCN	**349** and **362**[v,t]	**5.06** and **5.25**[v]	^{1}[βCN]* and ^{1}[βCH$^+$]*	**~385**[v]~390[t] **458**[v]	**0.68**[v]	**2.1**[v] **22.9**[v]	**0.08**[v]
		14	βCN	**349** and **362**	**5.15** and **5.25**	^{1}[βCN]*	**394**	**0.51**	**11.9**	—
2,9-diMe-nHo	—	4	βC-CH$_3^+$	**388**	**3.8**	^{1}[βC-CH$_3^+$]*	**462**	**0.74**	**25.9**	**0.16**
		9	βC-CH$_3^+$	**388**	**3.8**	^{1}[βC-CH$_3^+$]*	**462**	**0.74**	**25.9**	
		14	βC-CH$_3^+$	**388**	**3.8**	^{1}[βC-CH$_3^+$]*	**462**	**0.68**	**24.8**	—
Ho	p$K_a^{(N-2)}$: 7.34 (±0.03) [j], 7.37 (±0.04) [p,q], 7.7 [m]	4	βCH$^+$	**365**[v], 364[m], 364.4[p,r]	**4.45**[v]	^{1}[βCH$^+$]*	**431**, 430[m,z], 433.5[p,r], 440[xx]	**0.85**[v], 0.83[xx]	20.5[v], 21.2[t], 20.0[xx]	**0.09**[v]
	p$K_a^{(N-9)}$: **14.37** [o], 14.47 (±0.07)[j,k], 14.50	10	βCN	**335**[v] and **348**[v], 346[m], 346.8[p]	**4.80** and **4.50**[v]	^{1}[βCN]* and ^{1}[βCH$^+$]*	**374**, 378[m], 384[p] **431**, 433.5[p]	**0.47**[v]	0.6[z] 20.1[z]	**0.10**[v]
	(±0.07)[u], 14.6 (±0.1) [p,q], 20 (±1)[j,l]	13–14	βCN and	**336** and **347**; 336[p] and 349[p]		^{1}[βCA$^-$]*and ^{1}[βCZ]*	**482**[o], 440[j,u], 445[p] **496**[o], 483[m],	**0.23**, 0.056[u]	**9.1**	—
			βCA$^-$	**375**[o], 375[m], 374[p,s], 383[j], 375[u]	**3.39**[o], 3.83[j]		490.5[p,s], 491[j]			
2-Me-Ho	—	4	βC-CH$_3^+$	**368**, 366[j]	**3.5**	^{1}[βC-CH$_3^+$]*	**436**, 437[j]	**0.95**	**21.0**	**0.10**
	p$K_a^{(N-9)}$: **11.5** (±**0.1**), 11.2[j]	9	βC-CH$_3^+$	**368**	**3.5**	^{1}[βC-CH$_3^+$]*	**436**	**0.95**	**20.1**	
		13–14	βC-CH$_3$Z	**407**	**3.4**	^{1}[βC-CH$_3$Z]*	**503**, 511[j]	**0.11**	**6.9**	—
9-Me-Ho	p$K_a^{(N-2)}$: **6.6** (±**0.1**)	4	βCH$^+$	**378**[v]	**5.03**[v]	^{1}[βCH$^+$]*	**444**[v]	**0.93**[v]	**24.5**[v]	**0.09**[v]
	—	10	βCN	**346** and **360**[v]	**4.36** and **4.25**[v]	^{1}[βCN]* and ^{1}[βCH$^+$]*	**~374**[v] **444**[v]	**0.68**[v]	**2.5**[v] **23.8**[v]	**0.10**[v]
		14	βCN	**346** and **360**	**4.36** and **4.25**	^{1}[βCN]*	**374**	**0.43**	**7.1**	—
2,9-diMe-Ho	—	4	βC-CH$_3^+$	**382**	**4.1**	^{1}[βC-CH$_3^+$]*	**451**	**0.94**	**25.4**	**0.15**
		9	βC-CH$_3^+$	**382**	**4.1**	^{1}[βC-CH$_3^+$]*	**451**	**0.94**	**25.4**	
		13–14	βC-CH$_3^+$	**382**	**4.1**	^{1}[βC-CH$_3^+$]*	**451**	**0.83**	**24.6**	—

(continued)

Table 1. (continued)

Compound	pK_a in S_0[a]	pH	Species in S_0[b]	λ_{abs}/nm[c]	$\varepsilon(\lambda)/10^3$ M^{-1} cm^{-1}[d]	Species in S_1[b]	λ_F/nm[e]	Φ_F[f]	τ_F/ns[g]	Φ_Δ[h]
Ha	p$K_a^{(N-2)}$: 7.5[v], 7.73 (±0.03)[j], 7.7[x], 8.0[m]	4	βCH$^+$	**350**[v], 355[m]	**7.86**[v], 7.59[x]	^{1}[βCH$^+$]*	**417**, 418[m], 419[x], 425[xx]	**0.49**[v,w], 0.45[xx]	**7.0**, 7.1[w], 6.6[xx]	**0.22**[v]
	p$K_a^{(N-9)}$: **14.22**[o], 14.5[m], >14[x], 14.43 (±0.03)[j,k,u], 21 (±1)[j,l]	10	βCN	**325**[v] and **336**[v], 336[m], 326[x] and 338 (sh) [x]	**5.35**[v] and **4.68**[v] 5.62[x] and 4.90[x]	^{1}[βCN]* ^{1}[βCH$^+$]* and ^{1}[βCZ]*	**368**[o], 373[m], 370[x] **417**, 424[x] **~480**	**0.38**[v], 0.46[w] 0.34[w]	**0.44**, 0.41[w] **7.0**, 7.1[w]	**0.13**[v]
		13–14	βCN and βCA$^-$	**325** and **336** **363**[o], 370[m], 375 (sh) [x], 300[u]	**4.55**[o]	^{1}[βCA$^-$]* and ^{1}[βCZ]*	**468**[o],435[j, u], 430[x] **480**[o], 476[m], 482[j], 480[x]	**0.45,** 0.034[u]	**14.7** 14.3[w]	—
2-Me-Ha	— p$K_a^{(N-9)}$: **11.7 (±0.1)**, 11.2 (±0.1)[x], 11.5[m]	4	βC-CH$_3^+$	**360**, 360[m], 362[x]	**6.3**	^{1}[βC-CH$_3^+$]*	**422**, 422[m], 420[x], 433[xx]	**0.47**, 0.45[xx]	**7.0**, 6.5[xx]	**0.08**
		9	βC-CH$_3^+$	**360**, 362[x]	**6.3**	^{1}[βC-CH$_3^+$]*	**422**, 420[x]	**0.47**	**7.0**	
		13–14	βC-CH$_3$Z	**392**, 392[m], 398[x]	**5.3**	^{1}[βC-CH$_3$Z]*	**505**, 482[m], 485[x]	**0.24**	**11.9**	—
9-Me-Ha	p$K_a^{(N-2)}$: **7.1 (±0.1)**	4	βCH$^+$	**363**[y]	**6.83**[y]	^{1}[βCH$^+$]*	**430**[y]	**0.43**[y]	**9.1**[y]	**0.16**[y]
	—	10	βCN	**336** and **347**[y]	**5.24** and **4.92**[y]	^{1}[βCN]* and ^{1}[βCH$^+$]*	**~365**[y] **430**[y]	**0.35**[y]	**0.4**[y] **9.1**[y]	**0.15**[y]
		14	βCN	**336 and 347**	**5.24 and 4.92**	^{1}[βCN]*	**368**	**0.33**	**5.1**	—
2,9-diMe-Ha	—	4	βC-CH$_3^+$	**368**	**6.8**	^{1}[βC-CH$_3^+$]*	**434**	**0.45**	**8.7**	**0.16**
		9	βC-CH$_3^+$	**368**	**6.8**	^{1}[βC-CH$_3^+$]*	**434**	**0.45**	**8.7**	
		13	βC-CH$_3^+$	**368**	**6.8**	^{1}[βC-CH$_3^+$]*	**434**	**0.36**	**9.0**	—

[a]p$K_a^{(N-2)}$ and p$K_a^{(N-9)}$ represent the negative base 10 log of the acid dissociation constants (K_a) of pyridinic (N-2) and indolic (N-9) nitrogen atoms, respectively. [b]Main acid–base species present in the solution in the ground (S_0) or first electronic excited state (S_1) of βCs, under the pH condition indicated in the second column. [c]Maximum of the lowest-energy absorption band (λ_{abs}; ±2 nm). [d]Absorption coefficient (ε) at the maximum of the lowest-energy absorption band (error ≤ 5%). [e]Maximum of the emission band (λ_F) in aqueous solutions (±2 nm). [f]Fluorescence quantum yields (Φ_F) and [g]fluorescence lifetimes (τ_F) measured in air-equilibrated aqueous solutions (error ≤ 7%). [h]Quantum yield of singlet oxygen production (Φ_Δ) measured in air-equilibrated D_2O aqueous solutions (pD 7.7, error ± 10–15%). [i]From Ref. (70), measured from nHo (10^{-5} M) phosphate buffer solutions with 1% methanol. [j]From Ref. (54). [k]Data analyzed by the excess acidity (EA) methods. [l]Data analyzed by the Hammett acidity function (HAF). [m]From Ref. (55), measured from βC buffer solutions (0.1 M mixtures of acetic acid and sodium acetate for pH 3–4; l/15 M mixtures of Na_2HPO_4 and KH_2PO_4 for pH 5–8; 0.1 M mixtures of glycine and NaOH for pH 9–13. [n]From Ref. (71), measured from βC aqueous solutions. Note that pK_a^{N-9} of nHo is an estimated value. [o]Data deconvoluted from MCR-ALS and/or PARAFAC analysis. [p]From Ref. (73). [q]Measured in phosphate buffer at ionic strength <0.05. [r]Measured in water pH 0 (1 N, H_2SO_4). [s]Measured in water pH 14 (1 N, NaOH). [t]From Ref. (83) measured in aqueous solution; τ_F was measured from acidic (0.1 M, HCl) solutions. [u]From Ref. (74) measured in highly alkaline aqueous conditions (6.8 M KOH, at 25°C). [v]From Ref. (48), measured in aqueous solutions. [w]From Ref. (84), Φ_F of HaN was measured in benzene. [x]From Ref. (72), measured in aqueous solution. pK_a values measured in water containing 10% of methanol at ionic strength < 0.04; 2-methyl-harmanium tetrafluoroborate derivative was used. [y]From Ref. (45). [z]From Ref. (85). [xx]From Ref. (86), measured in water (0.1 N, H_2SO_4).

values are listed in Table 1. Briefly, data obtained herein show that

(1) 2-methyl-β-carbolinium iodide salts present similar K_a values, within experimental error, to those reported for the corresponding anhydrous bases (*i.e.* iodide-free 2-methyl-βCs) and/or 2-methyl-βCs salts stabilized with another counter ion (*i.e.* tetrafluoroborate) (53–55).

(2) The presence of the methyl group at N-2 enhances the acidity of indolic proton located at N-9 compared with those for the corresponding N-unsubstituted βCs: $pK_a^{(N-9)\ 2-Me-\beta Cs} \ll pK_a^{(N-9)\ \beta Cs}$ ($\Delta pK_a^{(N-9)} \sim 3 - 3.5$). In this case, the positive charge at the quaternary nitrogen atom (N-2) might behave as an additional factor for the delocalization/stabilization of the negative charge on N-9.

(3) pK_a values obtained on both groups of N-methyl derivatives (2-methyl- and 9-methyl-βCs) showed the same mild trend: $pK_a^{(N-9)\ 2-Me-Ha} > pK_a^{(N-9)\ 2-Me-Ho} > pK_a^{(N-9)\ 2-Me-nHo}$, whereas $pK_a^{(N-2)\ 9-Me-Ha} > pK_a^{(N-2)\ 9-Me-Ho} > pK_a^{(N-2)\ 9-Me-nHo}$. Briefly, the higher the substituents number present in the βC moiety and their electron donor character (-H, -CH_3 and –OCH_3, in nHo, Ho and Ha moieties, respectively), the lower the acidity of the -NH indolic group.

According to the above description, under physiologically relevant pH conditions, both protonated and neutral species of βCs and 9-methyl-βCs are present in the solution; whereas the cationic species of quaternary βCs (2-methyl- and 2,9-dimethyl-βCs) are the only dominant species. This fact correlates with the UV–visible absorption spectra. Briefly, quaternary βCs (2-Me-nHo and 2,9-diMe-nHo) show the same UV–visible absorption spectra when subject to pH conditions of 4.9 and 9.0–9.5 (Fig. 2b and d, respectively). In particular, quaternary βCs show a similar spectral pattern to that observed for protonated species of full-aromatic βCs such as nHo and 9-Me-nHo (see red lines in Fig. 2a and c, respectively). In both cases, the nonbonding (n) electron pair of the pyridine nitrogen is involved in the new σ-bond formed with the methyl group in 2-Me-nHo (76) and 2,9-diMe-nHo, or with the proton in $nHoH^+$ and 9-Me-$nHoH^+$. As a consequence, the overlapping between molecular orbitals is enhanced, leading to an extended π system (77), evidenced by the bathochromic shift in the absorption spectra of βCH^+ and $\beta C\text{-}CH_3^+$ with respect to βCN (red and blue lines, respectively, in Fig. 2).

Under highly alkaline conditions, nHo, as well as 2-Me-nHo, shows the presence of an additional acid–base species, due to the deprotonation of the indolic nitrogen (see black lines in Figs. 2a and b, respectively). Such alkaline species show a bathochromic shift, with respect to βCN and βCH^+ (or $\beta C\text{-}CH_3^+$), probably due to a higher electron density and interaction with the π system (extension of conjugation) of the negative charge at N-9. This effect is more evident in the case of 2-Me-nHo, where the positive charge located at N-2 might play a key role (withdrawing effect) (Scheme 2c). Spectra of N-Me-Ho and N-Me-Ha derivatives showed similar behavior (Figs. S4 and S5).

The addition of a N-methyl group into the βC moiety causes a bathochromic shift in all absorption bands (Fig. 3). This effect is, clearly, more evident when the substitution takes place at position 9, that is, a red shift of ~15 nm and ~5 nm is observed for 9-Me-βC and 2-Me-βCs, respectively. The addition of two

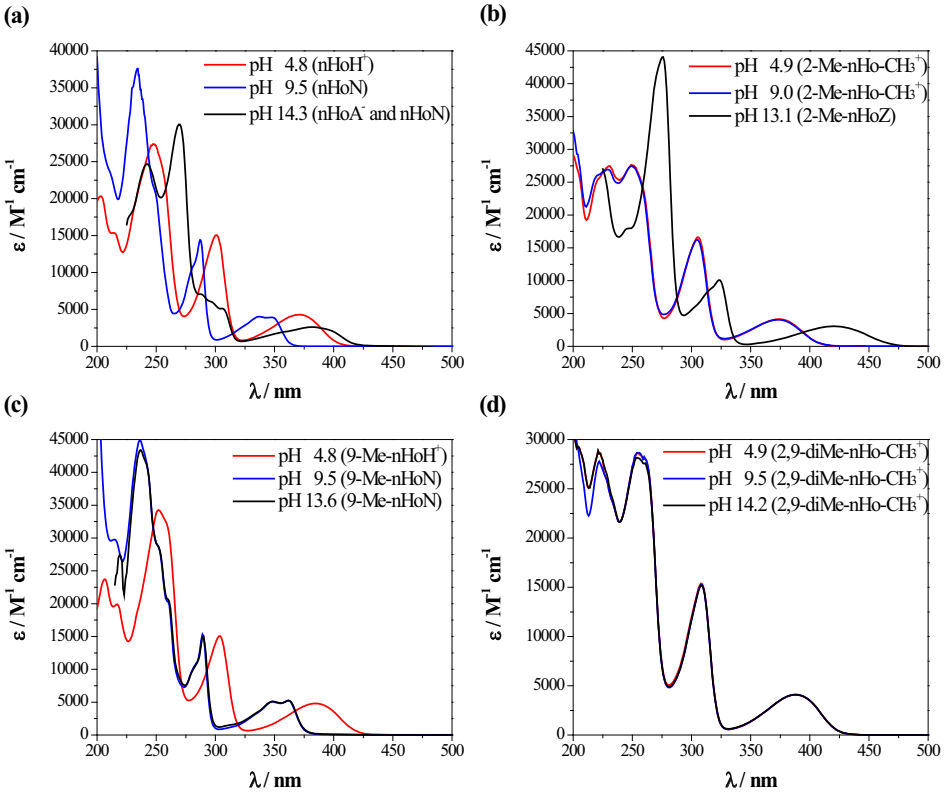

Figure 2. UV–visible absorption spectra of (a) nHo, (b) 2-Me-nHo, (c) 9-Me-nHo and (d) 2,9-diMe-nHo, recorded in aqueous solutions under three different pH conditions.

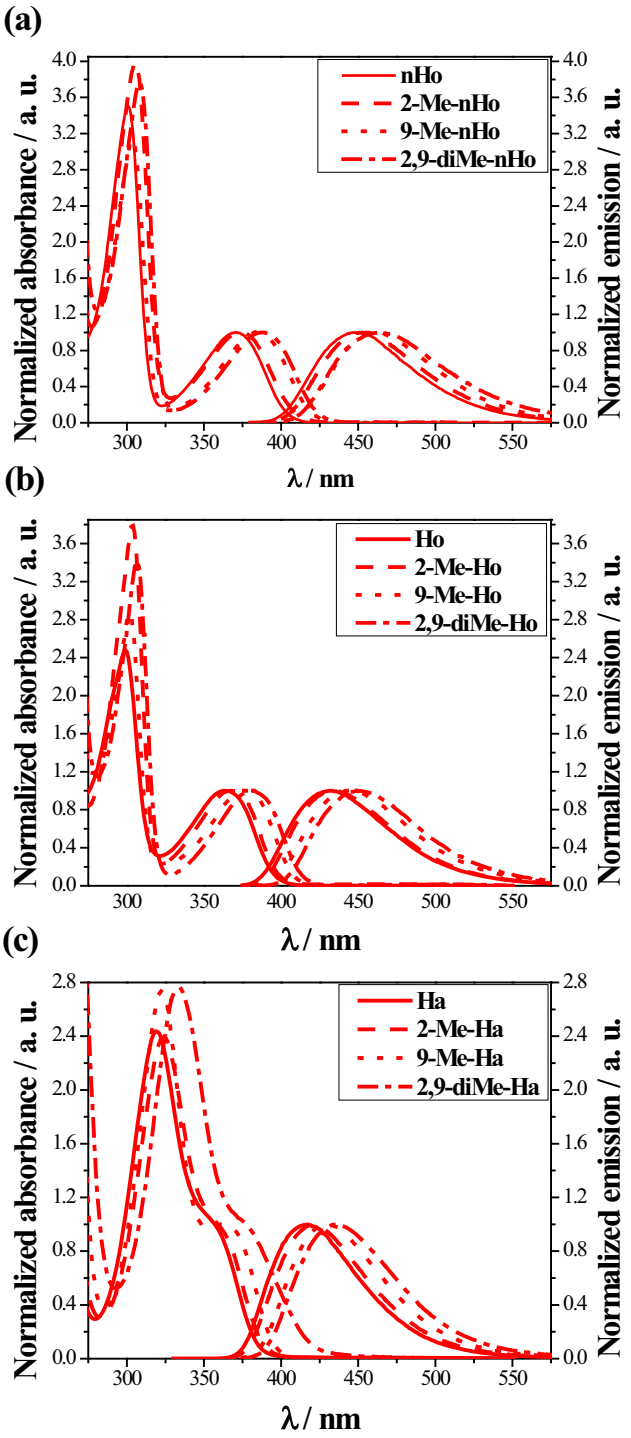

Figure 3. UV–visible absorption and emission normalized spectra of acidic (pH 4.8) aqueous solution of (a) nHo, 2-Me-nHo, 9-Me-nHo and 2,9-diMe-nHo, (b) Ho, 2-Me-Ho, 9-Me-Ho and 2,9-diMe-Ho and (c) Ha, 2-Me-Ha, 9-Me-Ha and 2,9-diMe-Ha.

N-methyl groups into the βC ring (2,9-diMe-βCs) showed an additive effect leading to a bathochromic shift of ~ 20 nm.

Chemometric analysis. It has been reported that the second pK_a of βCs is higher than 14; thus, from an experimental viewpoint, it is rather difficult to prepare aqueous solutions with pH values

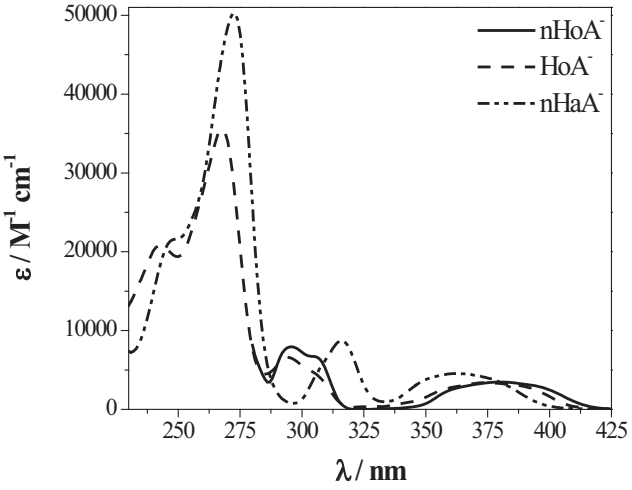

Figure 4. Optimized molar absorptivity of deconvoluted spectra of the anionic species of βCs (nHoA$^-$, HoA$^-$ and HaA$^-$) in aqueous solutions, obtained by the hybrid (hard-soft) modeling methodology.

high enough to estimate the spectrum of βCs anions (βCA$^-$), free of the interference of neutral species of βCs. Moreover, given the low contribution of the anion species to the absorbance matrix, the MCR-ALS algorithm could not achieve a deconvolution free of rotational ambiguities. Therefore, we have applied the hybrid (hard-soft) modeling methodology (Materials and Methods section), to obtain the pure spectra of βCA$^-$ (Fig. 4) as well as the optimal pK_a of the corresponding equilibrium (Table 1). The latter analysis yielded an optimal value of 14.08 ± 0.04; 14.37 ± 0.10; and 14.22 ± 0.10 for pK_a^{N9} of nHo, Ho and Ha, respectively, and the profiles are shown in Fig. S23. To the best of our knowledge, this is the first time that evidence is presented regarding this issue (*vide infra*).

Fluorescence spectroscopy

Steady-state fluorescence. Fluorescence emission and excitation spectra were recorded in aqueous solution under acidic (4.0 < pH < 5.0), low-alkaline (9.0 < pH < 10.0) and highly alkaline (13.0 < pH < 14.0) conditions (Figs. 5 and S6 – S9). For comparative purposes, normalized UV–visible absorption spectra were included in the same figures. The reported data in this section show that

(1) N-methyl-substitution of βC ring induces a bathochromic shift of the emission and excitation bands. This phenomenon is better represented in Fig. 3 where normalized emission spectra recorded under acidic aqueous solutions of N-methyl-βC are depicted. As in the case of UV–visible absorption spectra, this effect is more evident when the methyl group is attached in position N-9 than in position N-2. The highest bathochromic shift (~20 nm) observed in the cases of 2,9-dimethyl-βCs can be rationalized in terms of an additive effect induced by the two methyl groups attached to the βC ring.

(2) Under the whole pH range investigated (4–14), 2,9-diMe-βCs show only a quite intense emission band centered at ~460 nm. For all pH conditions and compounds, excitation spectra were coherent with the corresponding UV–vis absorption spectra (Figs. 5d, S8d and S9d). This behavior was expected as 2,9-diMe-βC derivatives show neither

indolic nor pyridinic acid–base equilibria. Therefore, upon excitation, the cationic species ($^1[\beta C\text{-}CH_3^+]^*$) would be the only emitting species.

(3) 2-Me-βCs show the expected behavior according to the acid–base equilibrium observed in the electronic ground state (S_0). These monosubstituted quaternary β-carbolinium salts may only exist as cations except under alkaline conditions (pH > 11) where the corresponding $\beta C\text{-}CH_3Z$ species is formed (Scheme 2c). As a consequence, excitation and emission spectra indicate that the recorded fluorescence may be ascribed to the first singlet excited states (S_1) of $^1[\beta C\text{-}CH_3^+]^*$ (λ_{em} ~ 460 nm) and $^1[\beta C\text{-}CH_3Z]^*$ (λ_{em} ~ 530 nm) for acidic/moderated alkaline (3 < pH < 10) and highly alkaline (pH > 12) 2-Me-βCs solutions, respectively (Figs. 5b and S6b – S9b). This result is in agreement with data reported by Sakurovs *et al.* for 2-Me-nHo (71).

(4) 9-Me-βCs show only two pH-dependent emitting species (Figs. 5c and S6c to S9c):

  (i) As it was already described for 9-Me-nHo and 9-Me-Ho (48), under acidic conditions (pH 5), only one emission band, centered at ~450 nm, was observed corresponding to the photoexcited N-pyridinic protonated cation $^1[\beta CH^+]^*$.

  (ii) Under low-alkaline conditions (pH 9), $^1[\beta CH^+]^*$ is the dominant emitting species. This fact might be a consequence, mainly, of the well-known enhanced basic character of the pyridinic nitrogen in the βC ring that takes place upon photoexcitation (70), yielding, in turn, $^1[\beta CH^+]^*$ as the main photoexcited species.

  (iii) On the contrary, photoexcitation of a highly alkaline (pH 13.5) solution of 9-Me-βC yields $^1[\beta CN]^*$ as the only electronically excited species. This outcome is aligned with the fact that, in the electronic ground state (S_0), these molecules show no additional acid–base equilibrium due to the presence of the methyl group at N-9 (*vide supra*). In addition, these data suggest that in S_1, $pK_a^{*(N-2)}$ for the pyridoindole main ring would be ranged between 9 and 13.5 in contrast with the value of 14.7 reported by Sakurovs *et al.* (by Förster relationship) (71).

(5) In the case of N-unsubstituted βCs, together with the pH effect on the excitation and emission spectra already described in the literature, new trends were observed under highly alkaline conditions (Figs. 5a and S6a and S9a) (48,70,72,73). Briefly, four different pH-dependent emitting species can be detected upon photoexcitation:

  (i) In acidic media (pH 4.0–5.0), $^1[\beta CH^+]^*$ is the only emitting species present in the solution, similarly as is observed in the case of 9-Me-βCH^+ (48,73).

  (ii) In the same way, under low-alkaline conditions (pH 9.0), two distinctive species, $^1[\beta CH^+]^*$ and $^1[\beta CN]^*$, were observed at ~450 nm (high relative intensity) and ~380 nm (low relative intensity), respectively (48). However, Ho and Ha showed an additional emission band overlapped the main emission band (see in Figs. S6a and S7a, respectively, the small increment of the emission intensity in the region of longer wavelengths,

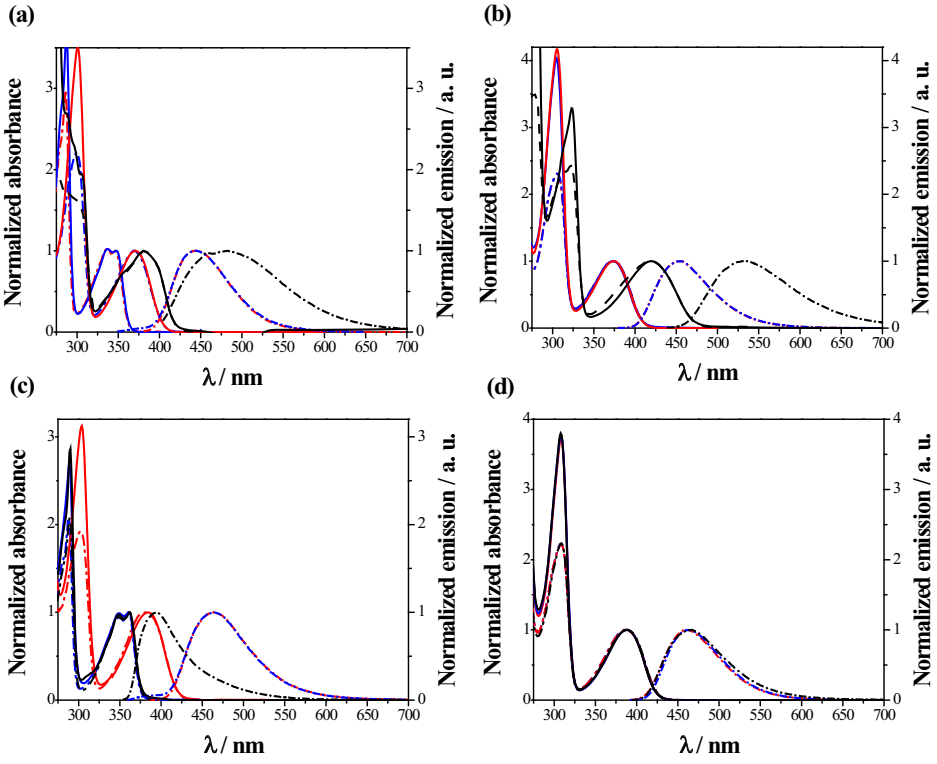

Figure 5. Normalized UV–visible absorption (solid lines), fluorescence emission (dotted lines) and excitation (dashed line) spectra of (a) nHo, (b) 2-Me-nHo, (c) 9-Me-nHo and (d) 2,9-diMe-nHo. Spectra were recorded in aqueous solutions under three different pH conditions: 4.8–4.8 (red lines), 9.0–9.5 (blue lines) and 13.0–14.5 (black lines). Emission and excitation spectra were recorded at the corresponding absorption and emission maximum, respectively (Table 1).

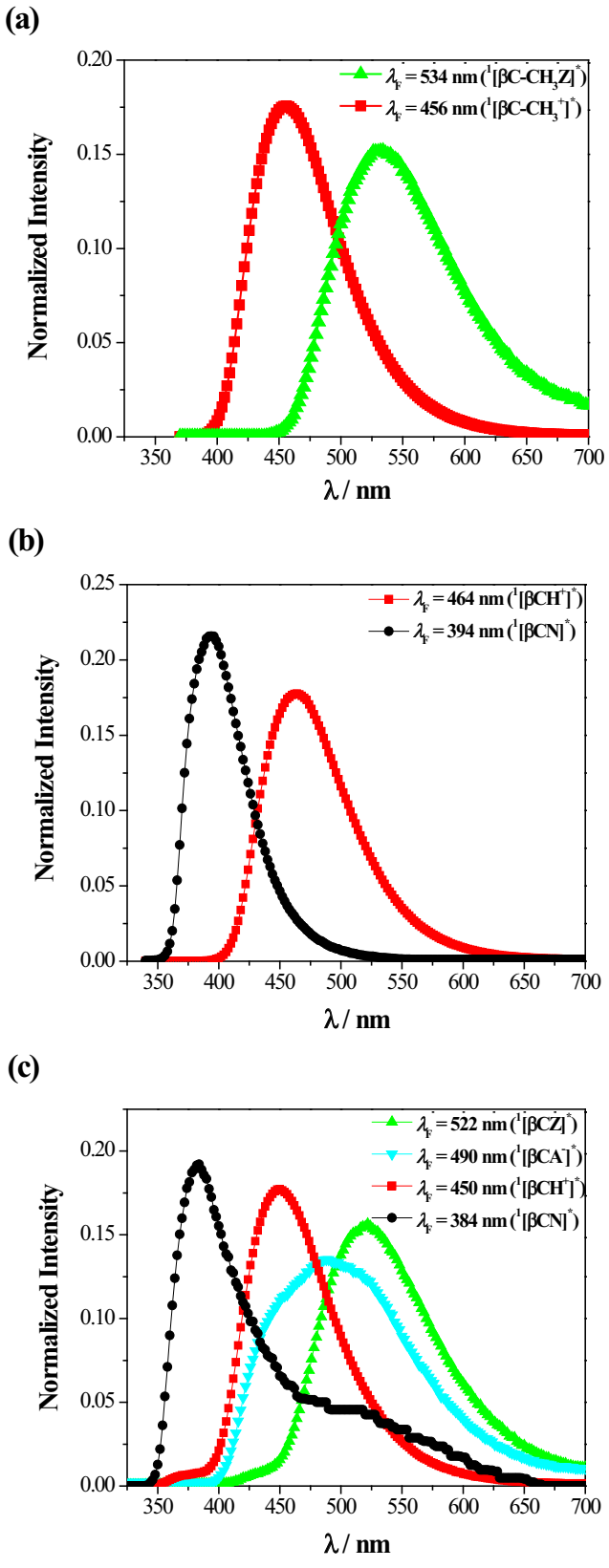

Figure 6. Normalized intensity of fluorescence emission spectra retrieved obtained with parallel factor analysis (PARAFAC) of acid–base titration of alkaline aqueous solution of: (a) 2-Me-nHo, (b) 9-Me-nHo and (c) nHo.

λ > 500 nm, depicted in the normalized emission spectra of pH 9 solutions). This effect is clearly more evident in the case of Ha. Sakurovs *et al.* (71) assigned the latter emission band to ^{1}[βCZ]*, which is also in agreement with data described above for alkaline 2-Me-βCs solutions.

(iii) On the contrary to the results published by Sakurovs *et al.* (71), upon photoexcitation of N-unsubstituted βCs in highly alkaline solutions, at the absorption maximum of βCA$^-$, two overlapped emission bands were observed, centered at ~490 nm and ~520 nm, respectively (Fig. 5a). In agreement with the results above described for the zwitterionic species of 2-Me-βCs and with the literature (71), the band centered at ~520 nm was assigned to ^{1}[βCZ]*. However, the emission band centered at ~490 nm was observed herein for the first time from βCs in highly alkaline solutions (pH > 13). This fact, in connection to the excitation spectra recorded at 490 nm, suggests that ^{1}[βCA$^-$]* would be the excited species responsible for the emission at this particular wavelength. Wolfbeis *et al.* (73) reported the emission of ^{1}[βCA$^-$]* only in the case of Ho. However, detailed absorption and excitation spectra of this species were not provided.

Note that, although N-unsubstituted βCs (nHo, Ho and Ha) have been extensively studied during the last 40 years, the photophysical and spectroscopic data reported in the literature for the species formed under highly alkaline pH conditions are not as conclusive and extensive as expected. In this context, data provided herein represent, to the best of our knowledge, the first systematic study providing direct evidence and full characterization of photoexcited anionic species (^{1}[βCA$^-$]*) of nHo, Ho and Ha.

Chemometric analysis of 3D emission-excitation fluorescence matrix. PARAFAC analysis was performed on the 3-way arrays constructed by stacking the EEMs of acid-base titrations of the indolic nitrogen (N-9) of nHo and 2-Me-nHo, as well as the pyridinic nitrogen (N-2) of 9-Me-nHo. The spectral shapes of the deconvoluted emission spectra are depicted in Fig. 6 (excitation spectra, data not shown, matched those of Fig. 5).

For 2-Me-nHo, all emission spectra recorded at different excitation wavelengths and pH values (3.8–14.0) were well reproduced, with a lack of fit (LOF) of 1.0%, using linear combinations of only two emission spectra, with intensity maxima located at 456 and 534 nm (Fig. 6a). The latter spectra are consistent with those ascribed in Fig. 5b to the emission of ^{1}[2-Me-nHo$^+$]* and ^{1}[2-Me-nHoZ]*, respectively. Similarly, for 9-Me-nHo, two spectral contributions, with intensity maxima at 464 and 394 nm (Fig. 6b), were required for fitting the entire set of emission spectra at different excitation wavelengths and pH values (2.7–14.2) (LOF = 1.5%). The latter spectra are consistent with those ascribed in Fig. 5c to the emission of ^{1}[9-Me-nHo$^+$]* and ^{1}[9-Me-nHoN]* species, respectively (*vide supra*).

In contrast, in the case of nHo, four independent spectral contributions were necessary for reproducing (LOF = 0.97%) the whole set of emission spectra obtained at different excitation wavelengths and pH values (10.5–14.5). The deconvoluted

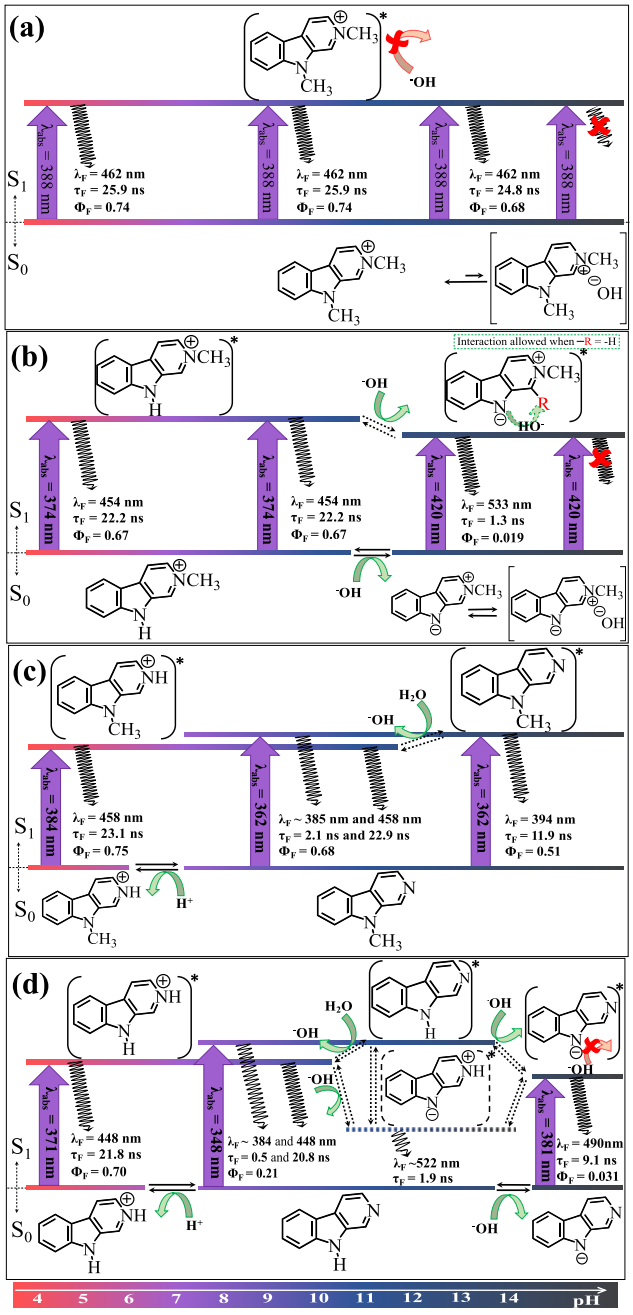

Scheme 3. Acid–base species of N-methyl-nHo: (a) 2,9-diMe-nHo; (b) 2-Me-nHo; and (c) 9-Me-nHo, as well as (d) N-unsubstituted nHo (as a representative example) present in the whole pH range investigated. Similar schemes can be drawn for Ho and Ha derivatives. In each case, drawings represent the dominant acid-base species present as a function of the pH according to the scale at the bottom. Green and red arrows represent, respectively, relevant and negligible processes for each compound under each pH conditions. Black solid and dashed arrows indicate processes or equilibria taking place in the ground and first electronic excited state, respectively.

emission spectra, with maxima at 522 nm, 490 nm, 450 nm and 384 nm, are presented in Fig. 6c. Comparison of the spectral shapes obtained for 2-Me-nHo and 9-Me-nHo with the contributions obtained for nHo suggests that the spectral contribution in red, green and black may be ascribed to ^{1}[nHo$^+$]*, ^{1}[nHoZ]* and ^{1}[nHoN]*, respectively. Noteworthy, the additional emission spectrum represented in cyan only contributes significantly to the total emission recorded at pH values above 14 and therefore may be ascribed to the emission of the anion species (^{1}[nHoA$^-$]*). The latter result is in line with those presented above (see Fluorescence spectroscopy—Steady-state fluorescence section).

To the best of our knowledge, the type of analysis presented here has never before been applied to the spectroscopic characterization of the excited states of *β*-carbolines. The chemometric tool used allowed the complete deconvolution of the fluorescence spectra associated with different acid–base species. Moreover, for the particular case of nHo, PARAFAC analysis of the recorded EEMs allowed our team to extract valuable conclusions concerning the of the system even under very alkaline conditions, where contradictory results have been reported in the literature owing to the overlap between the emission spectra of ^{1}[nHoZ]* and ^{1}[nHoA$^-$]*.

Time-resolved fluorescence. Fluorescence emission decay (Figs. S10 – S12) and lifetimes (τ_F) were determined for all the investigated compounds, in aqueous solutions (pH range 4.0–14.5). Average τ_F values obtained for each acid–base species of the investigated compounds are listed in Table 1. Furthermore, Tables S1–S3 show τ_F values obtained under all experimental conditions tested (pH, λ_{exc} and λ_{em}). Data reported herein can be summarized as follows:

(1) 2,9-diMe-*β*Cs show first-order fluorescence decays in the whole pH range investigated assigned to *β*C-CH$_3^+$ as the only species present in both S_0 and S_1 electronic states (*vide supra*). Mono-exponential fits lead to relatively high τ_F values: ~25 ns in the cases of 2,9-diMe-nHo and 2,9-diMe-Ho and ~9 ns for 2,9-diMe-Ha. For each compound, the observed values were the same, within experimental error, for all pH conditions. Thus, hydroxide anions do not quench S_1 of 2,9-diMe-*β*Cs.

When comparing the data described above with those previously reported for anhydrous bases and salts of 2-Me-nHo and 2-Me-Ha without iodide anion as counterion, our data show that iodide anion present in our experimental conditions neither interacts nor quenches S_1 of the quaternary *β*Cs herein studied.

(2) Mono-exponential decays with relative long-lived species were also observed for 2-Me-*β*Cs in acidic and low-alkaline aqueous solutions. However, decays obtained from pH 14 aqueous solutions yield shorter τ_F values (1.3–11.6 ns) than in acidic and low-alkaline pHs (~22 ns). The value obtained for 2-Me-nHo (1.3 ns) was the same, within experimental error, as that reported by Sakurovs *et al.* (71) for ^{1}[*β*C-CH$_3$Z]* as well as for the zwitterionic species of the N-unsubstituted nHo, ^{1}[(*β*CZ)]* (*vide infra*).

As it was described in point ***(1)***, those alkaloids with no exchangeable protons (*i.e.* 2,9-diMe-*β*Cs) did not show any quenching effect by the hydroxide anion, even at pH 14. Thus, the deactivation processes observed in the case of 2-Me-*β*Cs might involve the bimolecular interaction (most probably a proton transfer reaction) between photoexcited ^{1}[*β*C-CH$_3$Z]* and the solvent. In addition, the quite short τ_F value observed for the zwitterionic species of 2-Me-nHo might be a consequence of an additional interaction pathway between the solvent and/or the hydroxide anion with the hydrogen atom at C-1 (Scheme 3b).

(3) In accordance with the excitation and emission spectra described above, two different emitting species can be detected upon photoexcitation of 9-Me-βCs under acidic and/or low-alkaline conditions (pH range 4–10). Briefly, the shortest (< 0.5 ns) and the longest (~20 ns) lived species were assigned to $^1[\beta CN]^*$ and $^1[\beta CH^+]^*$, respectively. On the contrary, under highly alkaline conditions, only one long-lived (~10 ns) emitting species was observed. Taking into account the acid–base equilibrium depicted in Scheme 2, the latter emitting species was assigned to $^1[\beta CN]^*$, as βCN is the major absorbing species present in the solution under these experimental conditions.

It is worth mentioning that a quite strong pH-dependence was observed for τ_F values of $^1[\beta CN]^*$. This is in agreement with extremely fast proton transfer reaction between $^1[\beta CN]^*$ and the solvent to yield $^1[\beta CH^+]^*$ described above. Such a reaction would only take place to an appreciable extent under pH conditions lower than the pK_a*. In consequence, at pH 14, such a reaction would not represent a deactivation pathway of $^1[\beta CN]^*$.

(4) Fluorescence decays of alkaline (pH 14) species of N-unsubstituted βCs were also recorded. In the case of nHo, two emitting species were observed with τ_F values of 9.1 ns and 1.9 ns (Table 1). According to our data and to the literature, these two species were assigned to $^1[\beta CA^-]^*$ and $^1[\beta CZ]^*$, respectively. This is also in agreement with the fact that the βC anions ($^1[\beta CA^-]^*$) would show a lower interaction with hydroxide anions (due to repulsive interactions) than a positively charged $^1[\beta CZ]^*$, leading in the latter case to a fast decay.

(5) Under those conditions where protonated (or cationic) species are present, it is noticeable that the N-methylation induces a slight increase in the fluorescence lifetimes. Such an effect is more evident when substitution is at N-9 than N-2. Moreover, this increase is higher on di-N-substituted βCs suggesting that the effects are additive. These facts are in accordance with the increase in the Φ_F values (*vide infra*).

Quantum yields of fluorescence emission. The corresponding quantum yields of fluorescence (Φ_F) are listed in Table 1. In each case, values of Φ_F obtained using excitation wavelengths over the entire range of the lowest-energy absorption band were the same within experimental error (results not shown). Φ_F of N-unsubstituted βCs in acidic and low-alkaline conditions were previously reported (48). Briefly, Φ_F values of protonated species (βCH^+) of N-unsubstituted- and 9-Me-βCs (pH 4.8) are rather large (~0.70, ~0.90 and ~0.40 for nHo, Ho and Ha derivatives, respectively), and these values are larger than those obtained for the corresponding neutral forms (*i.e.* βCN, in pH 9.0 experiments). On the other hand, in the pH range 4–10, no pH effect on Φ_F of cationic 2-Me- and 2,9-diMe-βCs was observed. Note that Φ_F values, reported herein for the first time, were quite similar, within experimental error, to those obtained for βCH^+ of N-unsubstituted and 9-Me-βCs. In particular, the following trend was observed: $\Phi_F^{9\text{-Me-}\beta CH+} \sim \Phi_F^{2,9\text{-diMe-}\beta C} > \Phi_F^{\beta CH+} \sim \Phi_F^{2\text{-Me-}\beta C}$. Thus, the addition of a methyl group at position N-9 enhances radiative deactivation pathways by ~5–10%, whereas such effect is negligible or null when the substitution takes place at position N-2.

Under highly alkaline conditions, although relevant in almost all cases, Φ_F values obtained were smaller to those observed under acidic and/or low-alkaline pH conditions. Data listed in Table 1 show that Φ_F values were highly dependent on the chemical structure of the βC derivatives investigated. In the case of derivatives having exchangeable protons, the reported decrease in Φ_F might be a consequence of a deactivation of βCs' first electronic excited state (as is also suggested by the observed decrease in the corresponding τ_F) either by quenching by hydroxyl anions and/or by other competitive deactivation pathways such as proton transfer and/or tautomeric equilibria (Scheme 3). However, in the case of 2,9-diMe βCs that showed neither dynamic interaction between hydroxyl anion and their first electronic excited states nor exchangeable protons, a ground state complex between 2,9-diMe βCs and $^-$OH would be a reasonable explanation for the observed fact (Scheme 3a).

Quantum yield of singlet oxygen production

Singlet oxygen ($^1O_2$) is one of the so-called reactive oxygen species (ROS) that can be generated either through thermal, photosensitized or enzymatic processes. βCs are able to photosensitize $^1O_2$ formation, even upon two-photon excitation. The efficiency of ROS production depends on the chemical nature of the βC (45,47–49,51,78). In this context, the study of the capability of *nor*melinonine F, melinonine F and related N-methyl-β-carbolinium derivatives to photosensitize $^1O_2$ becomes relevant.

Quantum yields of singlet oxygen production (Φ_Δ) were determined for all 2-methyl- and 2,9-dimethyl-βC derivatives in D_2O under physiologically relevant pH conditions (Table 1). Representative phosphorescence decay traces of $^1O_2$, observed at 1270 nm after excitation of βCs, are depicted in Fig. S13. Briefly, quaternary βCs (2-Me-βCs and 2,9-diMe-βCs) show Φ_Δ values rather low ($0.08 < \Phi_\Delta < 0.16$) and similar, within experimental error, to those previously reported for the corresponding N-unsubstituted βC.

CONCLUSIONS

We report herein, for the first time, a complete and systematic spectroscopic and photophysical characterization of a selected group of βCs (nHo, Ho and Ha) and their N-methyl-derivatives (2-Me-, 9-Me- and 2,9-diMe-) in the pH range 3–14. Moreover, this work constitutes, to the best of our knowledge, the first systematic full characterization of anionic species of N-unsubstituted βCs ($nHoA^-$, HoA^-, and HaA^-), present under highly alkaline conditions. The main parameters obtained herein are summarized in Table 1, and all the acid–base species of N-methyl-βCs present in the whole pH range investigated are depicted in Scheme 3.

All the results provided in this report show, once more, the strong influences that pH as well as the nature and relative position of the substituents has on the photochemical and photophysical properties of β-carboline molecules. In consequence, each specific βC derivative deserves special attention, particularly for better assessing the correlation between alkaloid acid–base species and their physicochemical properties.

Furthermore, the results described herein contribute to our understanding of the photophysical behavior of βCs in biological environments and therefore contribute to further elucidate and/or forecast the roles played by these alkaloids in a wide range of biological systems:

(1) The most commonly accepted biological role of βCs is related to defense response mediated by ROS. However, their quite low efficiency of ROS production reported herein would suggest that defense response would not be a quite relevant process.
(2) ROS, and in particular singlet oxygen, can play a wide range of biological roles (79). At low doses, ROS would play a key role in ROS-mediated intracellular signaling (79–81). In this context, the role of βCs in phototriggered intracellular signaling processes (mediated by ROS and/or pH) should then be considered.
(3) Some βCs derivatives have been found in different tropical plants, subject to high doses of sunlight. Considering their capability to absorb the UVB fraction and UVA fraction of solar radiation, βCs could then act as endogenous protective agents, avoiding UV-induced damaging.
(4) Their extremely high efficiency of visible light emission makes these alkaloids good candidates as accessory pigments for light harvesting in photosynthesis, as well as fluorescent-induced pollinators attraction. Certainly, all these physiological roles deserve to be further investigated.

In addition, this study also provides reliable multivariate analysis (chemometry) for tracking bioactive compounds in natural product extracts. On the other hand, from a biotechnological point of view, the manuscript also provides valuable information. As naturally occurring secondary metabolites, βCs might represent an interesting alternative as fluorescent tracers (82), endowed with unique photophysical properties (able to sensing changes on the pH and oxygen partial pressure in intracellular spatial domains), that deserve to be explored in several fields of biology.

Moreover, these particular compounds allow for a great deal of chemical variability and can be fine-tuned to meet the requirements of a wide range of applications; that is, a simple methylation at N-2 and/or N-9 provides highly stable and fluorescent materials, even under extremely high pH conditions, useful as an example, for the development of light-emitting diodes, dyes sensitized solar cells (DSSC or Gräetzel fotovoltaic cells), among other possibilities.

Acknowledgements—The present work was partially supported by UBA (0055BA) and ANPCyT (PICT-2012-0072CO, 2012-0423 and 2015-0374). F.A.O.R-S. and T.S.D.L thank CONICET for their postdoctoral and doctoral research fellowships, respectively. F.S.G-E., M.R., R.E-B. and F.M.C. are research members of CONICET and P.D.G. is a research member of CIC-PBA. F.M.C. is also member of The TWAS Young Affiliate/Alumni Network (TYAN). The ESI-MS Q Exactive (Thermo Scientific) was supported by a grant from ANPCYT (PME2011-PPL2-0009, CEQUIBIEM, DQB, FCEN, UBA).

SUPPORTING INFORMATION

Additional Supporting Information may be found in the online version of this article:

Figures S1–S3. Thermal stability of (S1) nHo, 2-Me-nHo and 2,9-diMe-nHo, (S2) Ho, 2-Me-Ho and 2,9-diMe-Ho, and (S3) Ha, 2-Me-Ha and 2,9-diMe-Ha under acidic and alkaline conditions.

Figure S4–S5. UV-visible absorption spectra of (S4) harmane and (S5) harmine and their N-methyl derivatives.

Figure S6–S7. Normalized fluorescence emission spectra of (S6) harmane and (S7) harmine and their N-methyl derivatives.

Figure S8–S9. Normalized UV-visible absorption and fluorescence excitation spectra of (S8) harmane and (S9) harmine and their N-methyl derivatives.

Figure S10–S12. Fluorescence decays of (S10) *nor*harmane, (S11) harmane and (S12) harmine and their N-methyl derivatives.

Figure S13. Representative phosphorescence decay traces of singlet oxygen ($^1O_2$).

Figure S14–22. HRMS: Mass spectra for formula molecular and m.w. determination.

Figure S23. MRC-ALS analysis.

Table S1–S3. Average fluorescence lifetimes of (S1) *nor*harmane, (S2) harmane and (S3) harmine and their N-methyl derivatives.

REFERENCES

1. Larsen, L. K., R. E. Moore and G. M. L. Patterson (1994) β-Carbolines from the blue-green alga Dichothrix baueriana. *J. Nat. Prod.* **57**, 419–421.
2. Torreilles, J., M. C. Guerin and A. Previero (1985) Simple compounds with high pharmacologic potential: Beta-carbolines. Origins, syntheses, biological properties. *Biochimie* **67**, 929–947.
3. Adachi, J., Y. Mizoi, T. Naito, Y. Ogawa, Y. Uetani and I. Ninomiya (1991) Identification of tetrahydro-β-carboline-3-carboxylic acid in foodstuffs, human urine and human milk. *J. Nutr.* **121**, 646–652.
4. Manabe, S., J. Yuan, T. Takahashi and R. C. Urban Jr (1996) Age-related accumulation of 1-methyl-1,2,3,4-tetrahydro-beta-carboline-3-carboxylic acid in human lens. *Exp. Eye Res.* **63**, 179–186.
5. Pari, K., C. S. Sundari, S. Chandani and D. Balasubramanian (2000) β-carbolines that accumulate in human tissues may serve a protective role against oxidative stress. *J. Biol. Chem.* **275**, 2455–2462.
6. Spijkerman, R., R. van den Eijnden, D. van de Mheen, I. Bongers and D. Fekkes (2002) The impact of smoking and drinking on plasma levels of norharman. *Eur. Neuropsychopharmacol.* **12**, 61–71.
7. Breyer-Pfaff, U., G. Wiatr, I. Stevens, H. Jörg Gaertner, G. Mundle and K. Mann (1996) Elevated norharman plasma levels in alcoholic patients and controls resulting from tobacco smoking. *Life Sci.* **58**, 1425–1432.
8. Fekkes, D., A. Tuiten, I. Bom and L. Pepplinkhuizen (2001) Tryptophan: A precursor for the endogenous synthesis of norharman in man. *Neurosci. Lett.* **303**, 145–148.
9. Pfau, W. and K. Skog (2004) Exposure to β-carbolines norharman and harman. *J. Chromatogr. B Analyt. Technol. Biomed. Life Sci.* **802**, 115–126.
10. Hemmateenejad, B., A. Abbaspour, H. Maghami, R. Miri and M. R. Panjehshahin (2006) Partial least squares-based multivariate spectral calibration method for simultaneous determination of beta-carboline derivatives in Peganum harmala seed extracts. *Anal. Chim. Acta* **575**, 290–299.
11. Kam, T.-S., K.-M. Sim, T. Koyano and K. Komiyama (1999) Leishmanicidal alkaloids from Kopsia griffithii. *Phytochemistry* **50**, 75–79.
12. Caprasse, M., C. Coune and L. Angenot (1983) Isolement et structure de trois bases anhydronium du Strychnos usambarensis du Rwanda. *J. Pharm. Belg.* **38**, 135–139.
13. Kam, T.-S. and K.-M. Sim (1998) Alkaloids from Kopsia griffithii. *Phytochemistry* **47**, 145–147.
14. Downum, K. R. (1992) Light-activated plant defence. *New Phytol.* **122**, 401–420.
15. Rashid, M. A., K. R. Gustafson and M. R. Boyd (2001) New cytotoxic N-methylated β-carboline alkaloids from the marine ascidian Eudistoma gilboverde. *J. Nat. Prod.* **64**, 1454–1456.
16. Kearns, P. S., J. C. Coll and J. A. Rideout (1995) A β-carboline dimer from an Ascidian, Didemnum sp. *J. Nat. Prod.* **58**, 1075–1076.
17. Tadokoro, Y., T. Nishikawa, T. Ichimori, S. Matsunaga, M. J. Fujita and R. Sakai (2017) N-methyl-β-carbolinium salts and an N-methylated 8-oxoisoguanine as acetylcholinesterase inhibitors from a solitary Ascidian, *Cnemidocarpa irene*. *ACS Omega* **2**, 1074–1080.

18. Stachel, S. J., S. A. Stockwell and D. L. Van Vranken (1999) The fluorescence of scorpions and cataractogenesis. *Chem. Biol.* **6**, 531–539.
19. Siderhurst, M. S., D. M. James, C. D. Rithner, D. L. Dick and L. B. Bjostad (2005) Isolation and characterization of norharmane from Reticulitermes termites (Isoptera: Rhinotermitidae). *J. Econ. Entomol.* **98**, 1669–1678.
20. Cox, E. D. and J. M. Cook (1995) The Pictet-Spengler condensation: A new direction for an old reaction. *Chem. Rev.* **95**, 1797–1842.
21. Greiner, B., C. Fahndrich, S. Strauss and H. Rommelspacher (1983) Pharmacokinetics of tetrahydronorharmane (tetrahydro-β-carboline) in rats. *N-S Arch. Pharmacol.* **322**, 140–146.
22. Fekkes, D. and W. T. Bode (1993) Occurrence and partition of the β-carboline norharman in rat organs. *Life Sci.* **52**, 2045–2054.
23. Thomas, M. G., D. Sartini, M. Emanuelli, M. J. van Haren, N. I. Martin, D. M. Mountford, D. J. Barlow, F. Klamt, D. B. Ramsden, M. Reza and R. B. Parsons (2016) Nicotinamide *N*-methyltransferase catalyses the N-methylation of the endogenous β-carboline norharman: Evidence for a novel detoxification pathway. *Biochem. J.* **473**, 3253–3267.
24. Collins, M. A. and E. J. Neafsey (2000) b-Carboline analogues of MPP+ as environmental neurotoxins. In *Neurotoxic Factors in Parkinson's Disease and Related Disorders* (Edited by A. Storch and M. A. Collins), pp. 115–129. Kluwer Academic/Plenum Publishers, New York.
25. Gearhart, D. A., M. A. Collins, J. M. Lee and E. J. Neafsey (2000) Increased β-carboline 9N-methyltransferase activity in the frontal cortex in Parkinson's disease. *Neurobiol. Dis.* **7**, 201–211.
26. Gearhart, D. A., E. J. Neafsey and M. A. Collins (2002) Phenylethanolamine N-methyltransferase has β-carboline 2N-methyltransferase activity: Hypothetical relevance to Parkinson's disease. *Neurochem. Int.* **40**, 611–620.
27. Pavlovic, S., G. Schulze, C. Wernicke, R. Bonnet, G. Gille, L. Badiali, A. Kaminska, E. Lorenc-Koci, K. Ossowska and H. Rommelspacher (2006) 2,9-Dimethyl-β-carbolinium, a neurotoxin occurring in human brain, is a potent inducer of apoptosis as 1-methyl-4-phenylpyridinium. *Neuroscience* **139**, 1525–1537.
28. Hamann, J., H. Rommelspacher, A. Storch, H. Reichmann and G. Gille (2006) Neurotoxic mechanisms of 2,9-dimethyl-*β*-carbolinium ion in primary dopaminergic culture. *J. Neurochem.* **98**, 1185–1199.
29. Hamann, J., C. Wernicke, J. Lehmann, H. Reichmann, H. Rommelspacher and G. Gille (2008) 9-Methyl-β-carboline up-regulates the appearance of differentiated dopaminergic neurones in primary mesencephalic culture. *Neurochem. Int.* **52**, 688–700.
30. Alomar, M. L., F. A. Rasse-Suriani, A. Ganuza, V. M. Coceres, F. M. Cabrerizo and S. O. Angel (2013) In vitro evaluation of beta-carboline alkaloids as potential anti-Toxoplasma agents. *BMC Res. Notes* **6**, 193.
31. Di Giorgio, C., F. Delmas, E. Ollivier, R. Elias, G. Balansard and P. Timon-David (2004) In vitro activity of the *β*-carboline alkaloids harmane, harmine, and harmaline toward parasites of the species *Leishmania infantum*. *Exp. Parasitol.* **106**, 67–74.
32. Mishra, B. B., R. K. Singh, A. Srivastava, V. J. Tripathi and V. K. Tiwari (2009) Fighting against leishmaniasis: Search of alkaloids as future true potential anti-leishmanial agents. *Mini-Rev. Med. Chem.* **9**, 107–123.
33. Lala, S., S. Pramanick, S. Mukhopadhyay, S. Bandyopadhyay and M. K. Basu (2004) Harmine: Evaluation of its antileishmanial properties in various vesicular delivery systems. *J. Drug Target.* **12**, 165–175.
34. Gellis, A., A. Dumètre, G. Lanzada, S. Hutter, E. Ollivier, P. Vanelle and N. Azas (2012) Preparation and antiprotozoal evaluation of promising β-carboline alkaloids. *Biomed. Pharmacother.* **66**, 339–347.
35. McKenna, D. J. (2004) Clinical investigations of the therapeutic potential of ayahuasca: Rationale and regulatory challenges. *Pharmacol. Therapeut.* **102**, 111–129.
36. Tonin, L. T. D., M. R. Panice, C. V. Nakamura, K. J. P. Rocha, A. O. D. Santos, T. Ueda-Nakamura, W. F. D. Costa and M. H. Sarragiotto (2010) Antitrypanosomal and antileishmanial activities of novel N-alkyl-(1-phenylsubstituted-β-carboline)-3-carboxamides. *Biomed. Pharmacother.* **64**, 386–389.
37. Satou, T., A. Horiuchi, N. Akao, K. Koike, K. Fujita and T. Nikaido (2005) Toxocara canis: Search for a potential drug amongst *β*-carboline alkaloids-in vitro and mouse studies. *Exp. Parasitol.* **110**, 134–139.
38. Olmedo, G. M., L. Cerioni, M. M. González, F. M. Cabrerizo, V. A. Rapisarda and S. I. Volentini (2017) Antifungal activity of β-carbolines on *Penicillium digitatum* and *Botrytis cinerea*. *Food Microbiol.* **62**, 9–14.
39. Olmedo, G. M., L. Cerioni, M. M. González, F. M. Cabrerizo, S. I. Volentini and V. A. Rapisarda (2017) UVA photoactivation of harmol enhances its antifungal activity against the phytopathogens *Penicillium digitatum* and *Botrytis cinerea*. *Front. Microbiol.* **8**, 347. https://doi.org/10.3389/fmicb.2017.00347.
40. Van Baelen, G., S. Hostyn, L. Dhooghe, P. Tapolcsányi, P. Mátyus, G. Lemière, R. Dommisse, M. Kaiser, R. Brun, P. Cos, L. Maes, G. Hajós, Z. Riedl, I. Nagy, B. U. W. Maes and L. Pieters (2009) Structure-activity relationship of antiparasitic and cytotoxic indoloquinoline alkaloids, and their tricyclic and bicyclic analogues. *Bioorgan. Med. Chem.* **17**, 7209–7217.
41. Wright, C. W., J. D. Phillipson, S. O. Awe, G. C. Kirby, D. C. Warhurst, J. Quetin-Leclercq and L. Angenot (1996) Antimalarial activity of cryptolepine and some other anhydronium bases. *Phytother. Res.* **10**, 361–363.
42. Blom, J. F., T. Brütsch, D. Barbaras, Y. Bethuel, H. H. Locher, C. Hubschwerlen and K. Gademann (2006) Potent algicides based on the cyanobacterial alkaloid nostocarboline. *Org. Lett.* **8**, 737–740.
43. Gonzalez, M. M., M. Pellon-Maison, M. A. Ales-Gandolfo, M. R. Gonzalez-Baró, R. Erra-Balsells and F. M. Cabrerizo (2010) Photosensitized cleavage of plasmidic DNA by norharmane, a naturally occurring β-carboline. *Org. Biomol. Chem.* **8**, 2543–2552.
44. Gonzalez, M. M., M. Vignoni, M. Pellon-Maison, M. A. Ales-Gandolfo, M. R. Gonzalez-Baro, R. Erra-Balsells, B. Epe and F. M. Cabrerizo (2012) Photosensitization of DNA by β-carbolines: Kinetic analysis and photoproduct characterization. *Org. Biomol. Chem.* **10**, 1807–1819.
45. Vignoni, M., F. A. O. Rasse-Suriani, K. Butzbach, R. Erra-Balsells, B. Epe and F. M. Cabrerizo (2013) Mechanisms of DNA damage by photoexcited 9-methyl-*β*-carbolines. *Org. Biomol. Chem.* **11**, 5300–5309.
46. Caprasse, M. and C. Houssier (1983) Do planar alkaloids from Strychnos usambarensis intercalate into the DNA helix? *Biochimie* **65**, 157–167.
47. Gonzalez, M. M., M. L. Salum, Y. Gholipour, F. M. Cabrerizo and R. Erra-Balsells (2009) Photochemistry of norharmane in aqueous solution. *Photochem. Photobiol. Sci.* **8**, 1139–1149.
48. Gonzalez, M. M., J. Arnbjerg, M. Paula Denofrio, R. Erra-Balsells, P. R. Ogilby and F. M. Cabrerizo (2009) One- and two-photon excitation of β-carbolines in aqueous solution: pH-dependent spectroscopy, photochemistry, and photophysics. *J. Phys. Chem. A* **113**, 6648–6656.
49. Cabrerizo, F. M., J. Arnbjerg, M. P. Denofrio, R. Erra-Balsells and P. R. Ogilby (2010) Fluorescence quenching by oxygen: "Debunking" a classic rule. *ChemPhysChem* **11**, 796–798.
50. Hrsak, D., L. Holmegaard, A. S. Poulsen, N. H. List, J. Kongsted, M. P. Denofrio, R. Erra-Balsells, F. M. Cabrerizo, O. Christiansen and P. R. Ogilby (2015) Experimental and computational study of solvent effects on one- and two-photon absorption spectra of chlorinated harmines. *Phys. Chem. Chem. Phys.* **17**, 12090–12099.
51. Rasse-Suriani, F. A. O., M. Paula Denofrio, J. G. Yañuk, M. Micaela Gonzalez, E. Wolcan, M. Seifermann, R. Erra-Balsells and F. M. Cabrerizo (2016) Chemical and photochemical properties of chloroharmine derivatives in aqueous solutions. *Phys. Chem. Chem. Phys.* **18**, 886–900.
52. Tarzi, O. I., M. A. Ponce, F. M. Cabrerizo, S. M. Bonesi and R. Erra-Balsells (2005) Electronic spectroscopy of the β-carboline derivatives nitronorharmanes, nitroharmanes, nitroharmines and chloroharmines in homogeneous media and in solid matrix. *Arkivoc*, **vii**, 295–310.
53. Spenser, I. D. (1956) The structure of N_{β}-alkyl-β-carboline anhydrobases. *J. Chem. Soc. (Resumed)*, **704**, 3659–3663.
54. Balón, M., J. Hidalgo, P. Guardado, M. A. Muñoz and C. Carmona (1993) Acid-base and spectral properties of beta-carbolines. Part 2.

Dehydro and fully aromatic beta-carbolines. *J. Chem. Soc. Perk. T.* **2**, 99–104.
55. Vert, F. T., I. Z. Sanchez and A. O. Torrent (1983) Acidity constants of *β*-carbolines in the ground and excited singlet states. *J. Photochem.* **23**, 355–368.
56. Meech, S. R. and D. Phillips (1983) Photophysics of some common fluorescence standards. *J. Photochem.* **23**, 193–217.
57. Martí, C., O. Jürgens, O. Cuenca, M. Casals and S. Nonell (1996) Aromatic ketones as standards for singlet molecular oxygen $O_2(^1\Delta_g)$ photosensitization. Time-resolved photoacoustic and near-IR emission studies. *J. Photoch. Photobiol. A: Chem.* **97**, 11–18.
58. Gonzalez, M. M., M. P. Denofrio, F. S. Garcia Einschlag, C. A. Franca, R. Pis Diez, R. Erra-Balsells and F. M. Cabrerizo (2014) Determining the molecular basis for the pH-dependent interaction between 2′-deoxynucleotides and 9H-pyrido[3,4-b]indole in its ground and electronic excited states. *Phys. Chem. Chem. Phys.* **16**, 16547–16562.
59. de Juan, A., R. Gargallo, J. Jaumot and R. Tauler (2005) A graphical user-friendly interface for MCR-ALS: A new tool for Multivariate Curve Resolution in MATLAB. *Chemometr Intell Lab.* **76**, 101–110.
60. de Juan, A. and R. Tauler (2003) Chemometrics applied to unravel multicomponent processes and mixtures: Revisiting latest trends in multivariate resolution. *Anal. Chim. Acta* **500**, 195–210.
61. Gemperline, P. J. and E. Cash (2003) Advantages of soft versus hard constraints in self-modeling curve resolution problems. Alternating least squares with penalty functions. *Anal. Chem.* **75**, 4236–4243.
62. Lawton, W. H. and E. A. Sylvestre (1971) Self modeling curve resolution. *Technometrics* **13**, 617–633.
63. Tauler, R., A. Smilde and B. Kowalski (1995) Selectivity, local rank, three-way data analysis and ambiguity in multivariate curve resolution. *J. Chemometr.* **9**, 31–58.
64. Jaumot, J., R. Eritja and R. Gargallo (2011) Chemical equilibria studies using multivariate analysis methods. *Anal. Bioanal. Chem.* **399**, 1983–1997.
65. Andersen, C. M. and R. Bro (2003) Practical aspects of PARAFAC modeling of fluorescence excitation-emission data. *J. Chemometr.* **17**, 200–215.
66. Su, Y., F. Chen and Z. Liu (2015) Comparison of optical properties of chromophoric dissolved organic matter (CDOM) in alpine lakes above or below the tree line: Insights into sources of CDOM. *Photochem. Photobiol. Sci.* **14**, 1047–1062.
67. Ballesteros, S. G., M. Costante, R. Vicente, M. Mora, A. M. Amat, A. Arques, L. Carlos and F. S. G. Einschlag (2017) Humic-like substances from urban waste as auxiliaries for photo-Fenton treatment: A fluorescence EEM-PARAFAC study. *Photochem. Photobiol. Sci.* **16**, 38–45.
68. Ohno, T. (2002) Fluorescence inner-filtering correction for determining the humification index of dissolved organic matter. *Environ. Sci. Technol.* **36**, 742–746.
69. Bahram, M., R. Bro, C. Stedmon and A. Afkhami (2006) Handling of Rayleigh and Raman scatter for PARAFAC modeling of fluorescence data using interpolation. *J. Chemometr.* **20**, 99–105.
70. Draxler, S. and M. E. Lippitsch (1993) Excited-state acid-base kinetics and equilibria in norharman. *J. Phys. Chem.* **97**, 11493–11496.
71. Sakurovs, R. and K. P. Ghiggino (1982) Excited state proton transfer in β-carboline. *J. Photochem.* **18**, 1–8.
72. Wolfbeis, O. S. and E. Fuerlinger (1982) The pH-dependence of the absorption and fluorescence spectra of harmine and harmol: drastic differences in the tautomeric equilibria of ground and first excited singlet state. *Z. Phys. Chem.* **129**, 171–183.
73. Wolfbeis, O. S., E. Fürlinger and R. Wintersteiger (1982) Solvent- and pH-dependence of the absorption and fluorescence spectra of harman: Detection of three ground state and four excited state species. *Monatsh. Chem.* **113**, 509–517.
74. Balon, M., M. A. Muñoz and J. Hidalgo (1987) Fluorescence characteristics of β-carboline alkaloids in highly concentrated hydroxide solutions. *J. Photochem.* **36**, 193.
75. Coronilla, A. S., C. Carmona, M. A. Muñoz and M. Balón (2006) Ground state isomerism and dual emission of the β-carboline anhydrobase (N2-methyl-9H-pyrido[3,4-b]indole) in aprotic solvents. *Chem. Phys.* **327**, 70–76.
76. Sánchez-Coronilla, A., M. Balón, M. A. Muñoz and C. Carmona (2008) Influence of hydrogen bonding in the ground and the excited states of the isomers of the β-carboline anhydrobase (N_2-methyl-9H-pyrido[3,4-b]indole) in aprotic solvents. *Chem. Phys.* **344**, 72–78.
77. Dias, A., A. P. Varela, M. D. Miguel, A. L. Macanita and R. S. Beckers (1992) Beta.-Carboline photosensitizers. 1. Photophysics, kinetics and excited-state equilibria in organic solvents, and theoretical calculations. *J. Phys. Chem.* **96**, 10290.
78. Butzbach, K., F. A. O. Rasse-Suriani, M. M. Gonzalez, F. M. Cabrerizo and B. Epe (2016) Albumin-folate conjugates for drug-targeting in photodynamic therapy. *Photochem. Photobiol.* **92**, 611–619.
79. Ogilby, P. R. (2010) Singlet oxygen: There is indeed something new under the sun. *Chem. Soc. Rev.* **39**, 3181–3209.
80. Redmond, R. W. and I. E. Kochevar (2006) Spatially resolved cellular responses to singlet oxygen. *Photochem. Photobiol.* **82**, 1178–1186.
81. Finkel, T. (2011) Signal transduction by reactive oxygen species. *J. Cell Biol.* **194**, 7–15.
82. Duval, R. and C. Duplais (2017) Fluorescent natural products as probes and tracers in biology. *Nat. Prod. Reports* **34**, 161–193.
83. Sánchez Coronilla, A., C. Carmona, M. A. Muñoz and M. Balón (2010) Singlet excited state pyridinic deprotonation of the n_9-methyl-betacarboline cations in aqueous sodium hydroxide solutions. *J. Fluoresc.* **20**, 163–170.
84. Dias, A., A. P. Varela, M. da Graça Miguel, R. S. Becker, H. D. Burrows and A. L. Maçanita (1996) β-Carbolines. 2. Rate constants of proton transfer from multiexponential decays in the lowest singlet excited state of harmine in water as a function of pH. *J. Phys. Chem.* **100**, 17970–17977.
85. Reyman, D., M. H. Viñas, G. Tardajos and E. Mazario (2012) The impact of dihydrogen phosphate anions on the excited-state proton transfer of harmane. Effect of β-cyclodextrin on these photoreactions. *J. Phys. Chem. A* **116**, 207–214.
86. Pardo, A., D. Reyman, J. M. L. Poyato and F. Medina (1992) Some β-carboline derivatives as fluorescence standards. *JOL* **51**, 269–274.